

Research Journal of Pharmaceutical, Biological and Chemical Sciences

A Fluorescence Quenching Study of the Human Serum Albumin-Quercetin Complex by Addition of Cu (II), Ni (II) and Mn (II)

Chonghag Kim and Rubén M Savizky*

Department of Chemistry, The Cooper Union for the Advancement of Science and Art, New York, NY 10003

ABSTRACT

Fluorescence quenching studies were performed on a human serum albumin (HSA)-quercetin complex by adding three different divalent metal ions (Cu(II), Ni(II) and Mn(II)) to form a tertiary complex. Upon binding to human serum albumin, quercetin fluoresces after excitation at 295 or 450 nm. Two different quercetin moieties in the HSA-quercetin complex were observed to fluoresce, namely QC1 and QC2. The band shape of the QC1 emission peak was relatively sensitive to the nature of the quencher and the temperature. In contrast, the emission band of QC2 was not shifted upon changing the temperature, but was shifted if tryptophan or tyrosine emission were quenched. The divalent metal ions acted as quenchers for both QC1 and QC2 emissions. Results were analyzed using the Stern-Volmer relationship by plotting the relative intensity vs. the quencher concentration. From the Stern-Volmer plots, QC1 and QC2 emission peaks were seen to be quenched by collisional quenching, with a minor contribution due to static quenching in the presence of Cu(II). When Mn(II) was added to the complex, QC1 was quenched by collision only while QC2 was quenched by the combination of both mechanisms, although collisional quenching was the dominant mechanism. In the case of QC2 quenching by Ni(II), the interpretation of the Stern-Volmer relationship was difficult since changing the temperature did not alter the ratio of the fluorescence intensity in the absence and presence of the quencher (F_0/F) at the original temperature. Even though the change was small in the Stern-Volmer plots, it can be stated that the QC2 emission band is possibly due to complex formation with Ni (II).

Keywords: Human serum albumin, quercetin, fluorescence quenching, Stern-Volmer

*Corresponding author

INTRODUCTION

Human serum albumin (HSA) is the most abundant protein in blood serum, making up about 60% of the total serum protein concentration. The main functions of HSA include maintaining osmotic blood pressure, serving as a depot protein, and transporting diverse endogenous and exogenous ligands including fatty acids, bilirubin, drug molecules, and metal ions [1]. Figure 1 shows the three-dimensional structure of HSA [2]. HSA has only one tryptophan at position 214, which fluoresces upon excitation. HSA is well-known to be flexible and therefore able to bind small molecules. Cu(II) and Ni(II) are found to bind to the N-terminus with association constants (K_A) of 2×10^{16} and $4 \times 10^9 \text{ M}^{-1}$, respectively [3]. It is known that histidine 3 plays a crucial role in binding, but it has also been reported that histidines 105, 146, 247 and aspartate 249 are responsible for binding Cd(II) and Zn(II) [4]. Furthermore, a K_A value of $2.4 \times 10^4 \text{ M}^{-1}$ has been reported for Mn(II) in the same binding site using ^{17}O relaxation measurements [4,5].



Figure 1: Three-dimensional crystal structure of human serum albumin (pdb file 1AO6) [2]. This figure was produced with the program Rasmol.

Quercetin (3,5,7,3',4'-pentahydroxyflavone, Figure 2) exhibits some of the common physiological activities of flavonoids, such as protection of low-density lipoprotein, prevention of platelet aggregation, relaxation of cardiovascular smooth muscle, antiviral and carcinostatic properties, antioxidant activity, and anti-inflammatory activity [6,7]. Quercetin contains several substituents including a carbonyl group at carbon 4 and hydroxyl groups at the 3, 5, 7, 3' and 4' positions. These substituents make quercetin one of the most biologically active flavonoids.

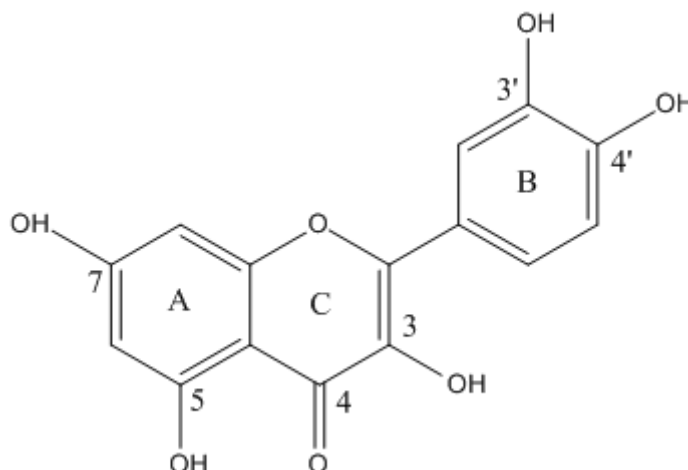


Figure 2: Chemical structure of quercetin.

A fluorescence excitation spectrum represents the relative efficiencies of different wavelengths of incident light to excite most fluorophores. However, due to the emitted light having lower energy, emission typically occurs at longer wavelengths than excitation. Blue- or red-shifted emission may occur if the fluorophore environment changes. For example, the more buried residues in a protein's structure have the more blue-shifted emission. In a fluorescence spectrum, there are a number of properties that are considered significant, such as fluorescence intensity, wavelength maximum, band shape, fluorescence lifetimes, and anisotropy [8,9]. Fluorescence is especially useful at low concentration, because fluorescence intensity has a linear relationship with the concentration of the emitting species.

Quenching measurements are a valuable source to reveal the accessibility of fluorophores to quenchers because a decrease in intensity at a specific wavelength is observed in emission spectra upon quencher addition. However, there are a number of quenching mechanisms available. By the addition of other molecules, excited fluorophores experience energy loss due to collisions between molecules. In the case of collisional (dynamic) quenching, the quencher must diffuse to the fluorophore and contact the excited fluorophore physically, which returns to the ground state after the energy of the excitation previously absorbed is taken away by the quencher. In a simple case of dynamic quenching, the following three-state scheme can be written: $F^* + Q \rightleftharpoons F^*:Q \rightarrow F + Q$, where F^* and F are the fluorophore in its excited and ground states, respectively, Q is the quencher molecule, and $F^*:Q$ represents a complex between the excited fluorophore and the quencher. When the quencher binds to a fluorescent molecule, quenching due to the ground-state complex formation between two molecules

occurs. Therefore, static quenching is a valuable source of information about the binding between the fluorescent molecule and the quencher [10]. In a simple case of static quenching, the following two-state scheme can be written: $F+Q \rightleftharpoons F:Q$, where F is the fluorophore in its ground state, Q is the quencher molecule, and F:Q represents a complex between the fluorophore and the quencher.

Transition metal-quercetin complexes have been studied using fluorescence spectroscopy to investigate the structures of these complexes [8]. There are also several possible metal ion-complexing moieties, such as the 3',4'-dihydroxyl group on the B-ring and the 3- or 5-hydroxyl and 4-carbonyl group on the A- or C-rings [9, 10]. However, the ratio of metal to ligand and the location of the metal ion binding sites have not been exactly found and remain ambiguous, depending on the environment and the type of metal ion. When quercetin is absorbed in the human body, HSA is the main carrier protein in blood plasma [11]. Quercetin probably binds to site IIA, where Trp214 is located [12].

MATERIALS AND METHODS

All chemicals used in the experiment were analytical standard reagents. Methanol (>99.8%, anhydrous), quercetin ($\geq 98\%$, anhydrous), copper(II) chloride ($\geq 99.995\%$, trace metal basis, anhydrous), nickel(II) chloride ($\geq 99.99\%$, trace metal basis, anhydrous), manganese(II) chloride ($\geq 99.999\%$, trace metal basis, -10 mesh, anhydrous), Trizma[®] hydrochloride (Tris-HCl) buffer solution (pH 7.4, 1M) and albumin from human serum (lyophilized powder, $\geq 97\%$, agarose gel electrophoresis) were purchased from Sigma Aldrich Co. Assurance Grade ASTM Type I Water Blank (AA Grade water) purchased from SpexCertiprep was used throughout the experiments.

Fluorescence spectra were recorded by a Cary Eclipse Fluorescence Spectrophotometer using a 1.00 cm quartz cell and a slit width of 5 nm. The excitation spectra were taken without setting an emission wavelength by using the "zeroth order" option. The following settings were used for emission spectra recorded: excitation wavelength of 276 nm, emission range of 280 to 400 nm; excitation wavelength of 295 nm, emission range of 300 to 575 nm; excitation wavelength of 380 nm, emission range of 480 to 580 nm; excitation wavelength of 450 nm, emission range of 460 to 600 nm. The photomultiplier detector voltage was set to be 660V. The excitation filter and emission filter were set to be auto and open, respectively. For temperature-controlled experiments, a single-cell Peltier block was used. The temperature range was between 20 and 30 °C. The recorded spectra were smoothed by the Savitzky-Golay method, using a factor of 5 and an interpolated factor of 5.

Experimental

1 M Tris-HCl buffer solution at pH 7.4 was diluted with AA Grade water to make a 50 mM Tris-HCl buffer solution. Dilution of the buffer solution did not affect the pH, therefore no further adjustment was made. A stock solution of HSA was prepared by dissolving 1 g of HSA in 25 mL of 50 mM Tris-HCl buffer, which was kept at -20 °C. A 7.5 mM quercetin solution was

prepared by dissolving 0.0113 g of quercetin in 5 mL of methanol and stored in the dark at room temperature. 75 mM Cu(II) stock solutions were prepared by dissolving 0.0504 g of copper(II) chloride in 5 mL of AA Grade water on the day of the experiment and diluted to 7.5 mM before fluorescence spectra were recorded. 75 mM Ni(II) stock solutions were prepared by dissolving 0.0460 g of nickel(II) chloride in 5 mL of AA Grade water on the day of the experiment and diluted to 7.5 mM before fluorescence spectra were recorded. 150 mM Mn(II) stock solutions were prepared by dissolving 0.0944 g of manganese(II) chloride in 5 mL of AA Grade water on the day of the experiment and diluted to a concentration of 15 mM before fluorescence spectra were recorded.

Factors affecting fluorescence emission spectra and quantum yields include solvent polarity, viscosity, rate of solvent relaxation, rigidity of the local environment, probe conformational changes, internal charge transfer, proton transfer and excited state reactions, probe-probe interactions, and changes in radiative and non-radiative decay rates [13]. The effects of the solvent on fluorescence spectra are too complex to know which effect is dominant in a specific system. Fluorescence spectra were recorded in various environments including different solvents, temperature, excitation wavelengths, and spectral types. In order to avoid the solvent effect on tryptophan fluorescence, the final volume upon quencher addition was set to be 20 μ L of methanol or water. The added methanol and water volume did not exceed 0.8% of the total volume of the binary mixture. In the case of mixing three components (HSA, quercetin, and a metal ion) the maximum addition of methanol and water was set to be 5 and 20 μ L, respectively, and did not exceed 1% of the total volume of the tertiary mixture. Finding the solvent effect on tryptophan fluorescence, spectra were recorded after water or methanol was added into 2.5 mL of a 15 μ M HSA solution by increments of 5 μ L, up to a total of 20 μ L.

5 μ L of a 7.5 mM quercetin solution was added into 2.5 mL of a 30 μ M HSA solution. 5 μ L of a 7.5 mM solution of a quencher, such as Cu(II) or Ni(II), was added into 2.5 mL of a 30 μ M HSA solution. Each quencher addition increased the quencher concentration by 15 μ M in the solution. In the case of Mn(II), the stock solution was set to be 15 mM; therefore each addition resulted in a 30 μ M increase of the quencher concentration. Since the reaction time for the interaction of the HSA-quercetin complex with Cu(II), Ni(II) or Mn(II) was not defined clearly in the literature, the time interval for recording spectra was set to be as consistent as possible.

RESULTS AND DISCUSSION

Initially, solvent effects were investigated. Adding solvents would change the local environment near a fluorophore in the protein. In this study, the maximum volume of solvent added in an HSA-quercetin solution was 20 μ L of water or methanol, respectively. Addition of water changed the excitation peak near 275 nm (due to both tryptophan and tyrosine excitation) by less than 1% of the total fluorescence intensity, thus resulting in negligible effects (Figure 3a). The changes upon addition of methanol are shown in Figure 3b. The excitation intensity fluctuated near 280 nm because tryptophan fluorescence is extremely sensitive to its local environment. In protein structure, a red-shift in emission spectra occurs if a fluorophore is

exposed, while a blue-shift occurs if a fluorophore is buried. As was observed with water, methanol addition changed the emission peak by less than 1% of the total fluorescence intensity, thus resulting in a negligible effect on emission.

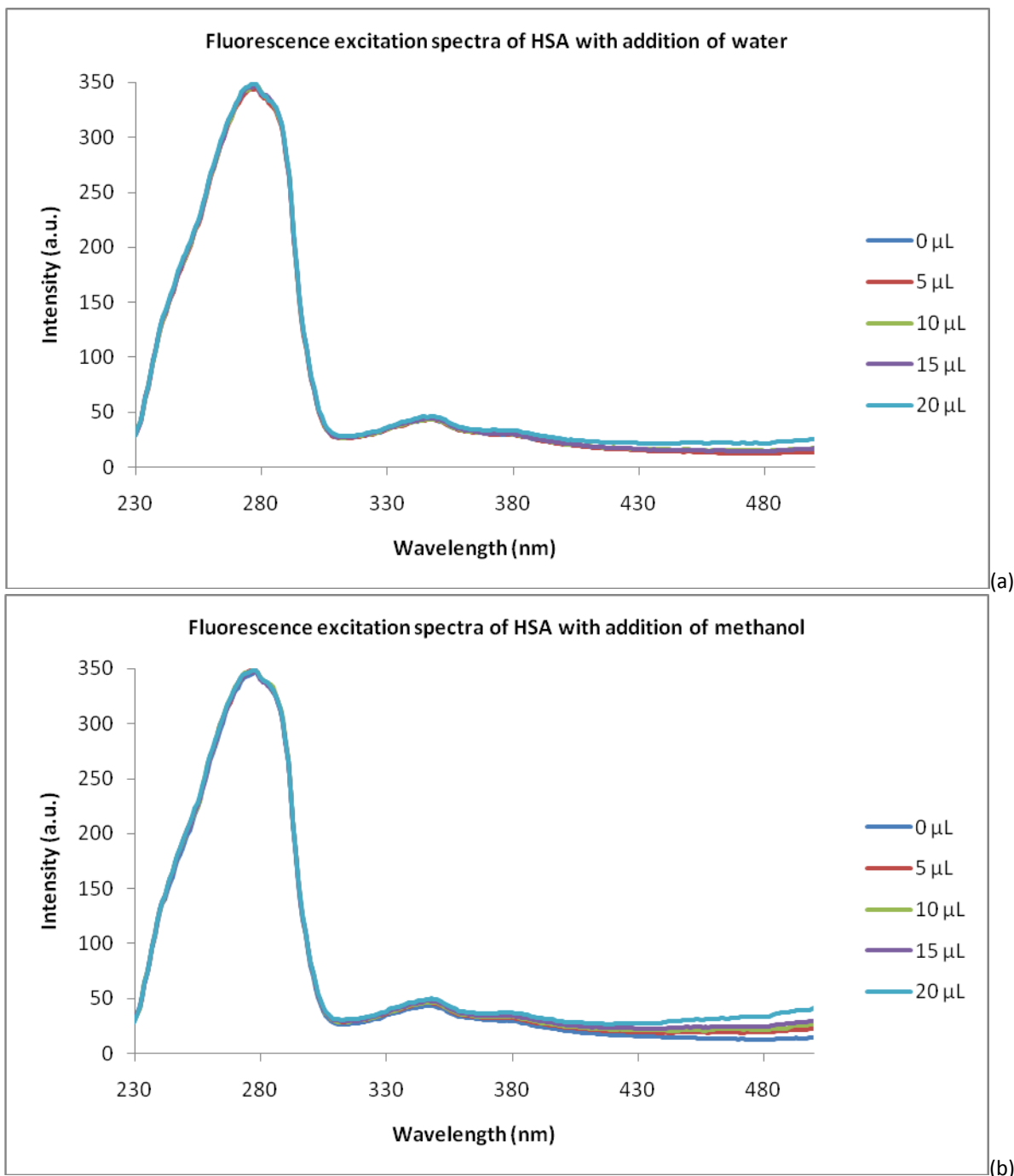
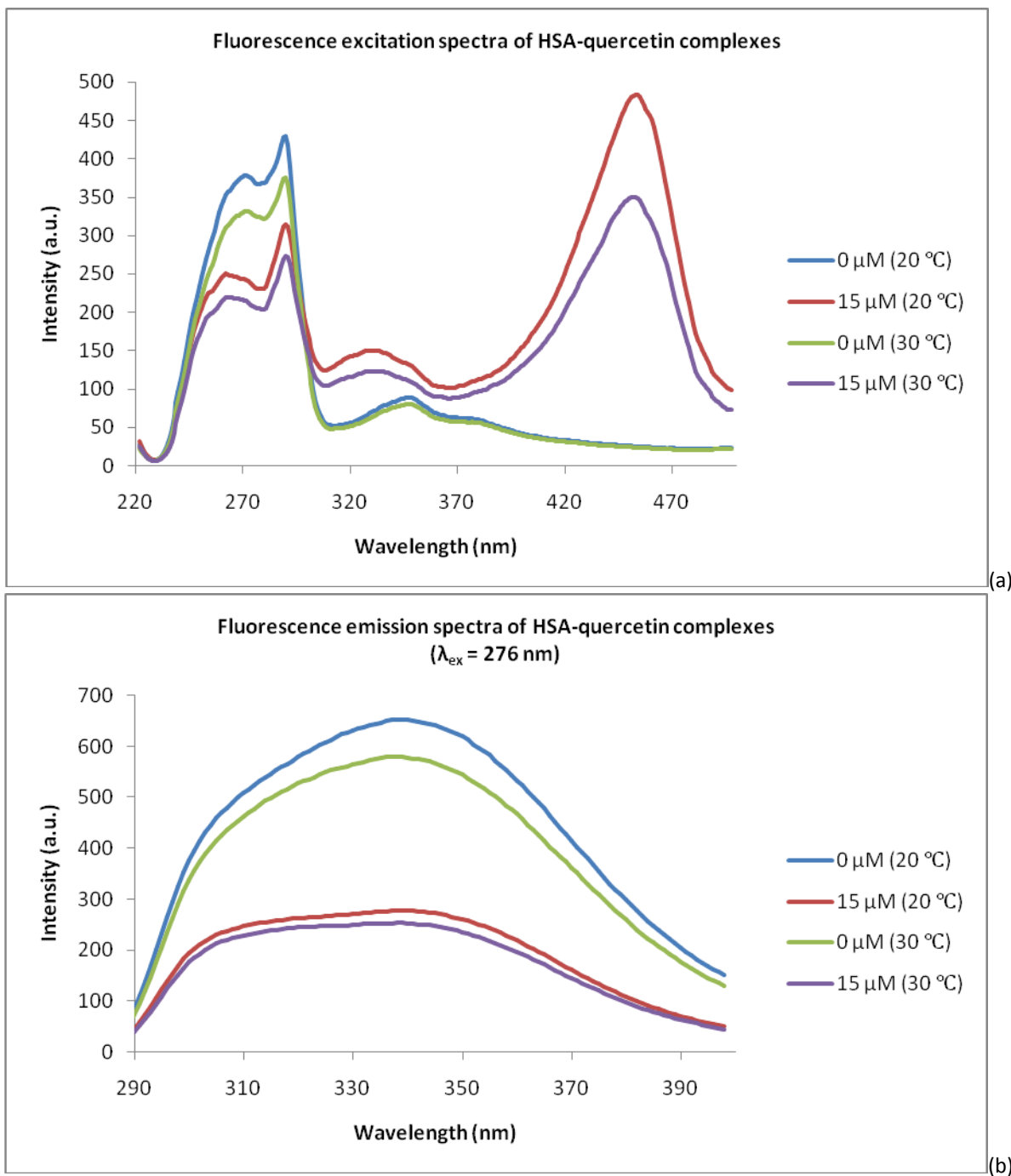
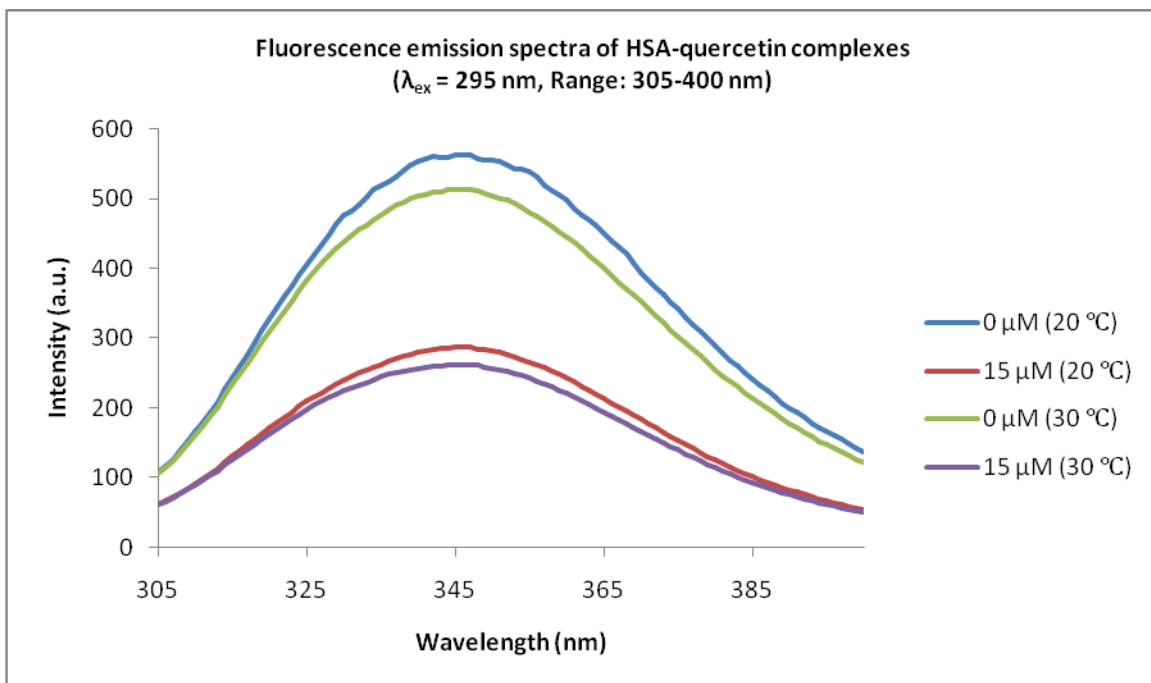


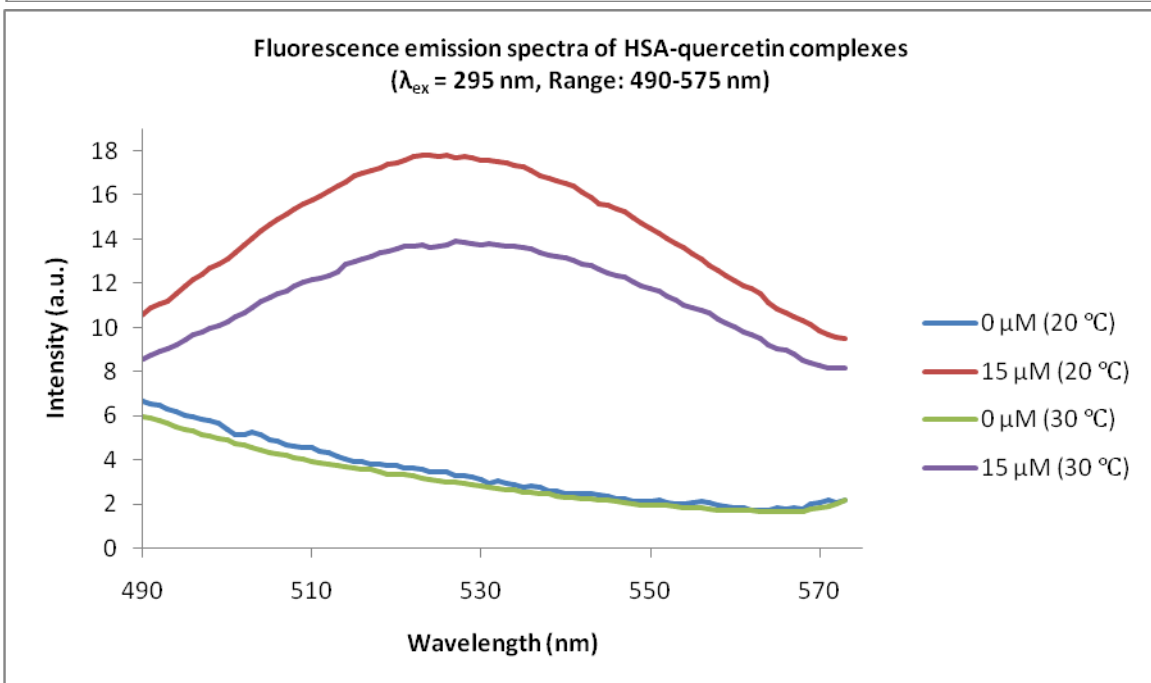
Figure 3: Solvent effects on HSA fluorescence spectra. All measurements were performed by adding 5 μ L increments of the solvent to 2.5 mL of 15 μ M HSA in 50 mM Tris-HCl buffer with a scan rate of 300 nm/min. (a) Addition of water; (b) addition of methanol.

Fluorescence quenching studies on 30 μ M HSA by different quenchers were performed at 20 and 30 °C. The addition of quercetin decreased both tyrosine and tryptophan emission by approximately 35 and 25%, respectively. The broad band shift and an increase in excitation intensity were observed near 330 nm in Figure 4a. These alterations were observed due to a change in the quercetin structure and indicate the formation of a ground-state complex between HSA and quercetin. A strong band with an excitation maximum near 450 nm corresponds to the quercetin moiety participating in complex formation with HSA [16]. By increasing the temperature, excitation intensities were significantly decreased. This is possibly due to the relation between temperature and viscosity. In the case of a fluorophore bound to a biomolecule, a decrease in local viscosity contributes to decreased fluorescence intensities [10]. As temperature increases, solvent viscosity decreases, resulting in a decrease in intensities. Both tyrosine and tryptophan emission were significantly quenched upon the addition of 15 μ M quercetin at 20 and 30 °C, as seen in Figure 4b. Previous studies indicate that quercetin may bind at a hydrophobic region, where complex formation is possibly due to a charged side chain, at two different sites near tryptophan 214 [16]. Therefore, the decrease in intensity around 340 nm (tryptophan emission) was larger than the decrease in intensity around 310 nm (tyrosine emission). Only the tryptophan residue was excited upon excitation at 295 nm in Figure 4c. The emission spectra clearly indicate that quercetin is a strong quencher of tryptophan 214. Increasing the temperature quenched an emission peak around 345 nm more significantly. Previous studies indicate that quercetin has maximum absorption at a wavelength of 375 nm in UV/Vis spectra collected in ethanol at room temperature [17]. Therefore, spectral overlap can be observed by a tryptophan emission spectrum (donor) with a maximum near 345 nm and the quercetin absorption spectrum (acceptor) with a maximum near 375 nm. A number of previous studies reported that an emission maximum around 530 nm upon an excitation at 295 nm is due to resonance energy transfer between quercetin and tryptophan 214 [14, 16-18]. Surprisingly, emission spectra upon 380 nm are almost identical in terms of band shape and fluorescence intensity (Figures 4d and e). Therefore, it is highly possible that light with wavelengths of 295 and 380 nm excites the same quercetin-fluorophore. However, the quercetin moiety in the HSA-quercetin complex fluoresces upon excitation at 450 nm, as seen in Figure 4f. This brings up an interesting question: is the quercetin moiety in the complex structure, which is responsible for emission upon an excitation at 450 nm, the same fluorophore that is excited by light with wavelengths of 295 or 380 nm?





(c)



(d)

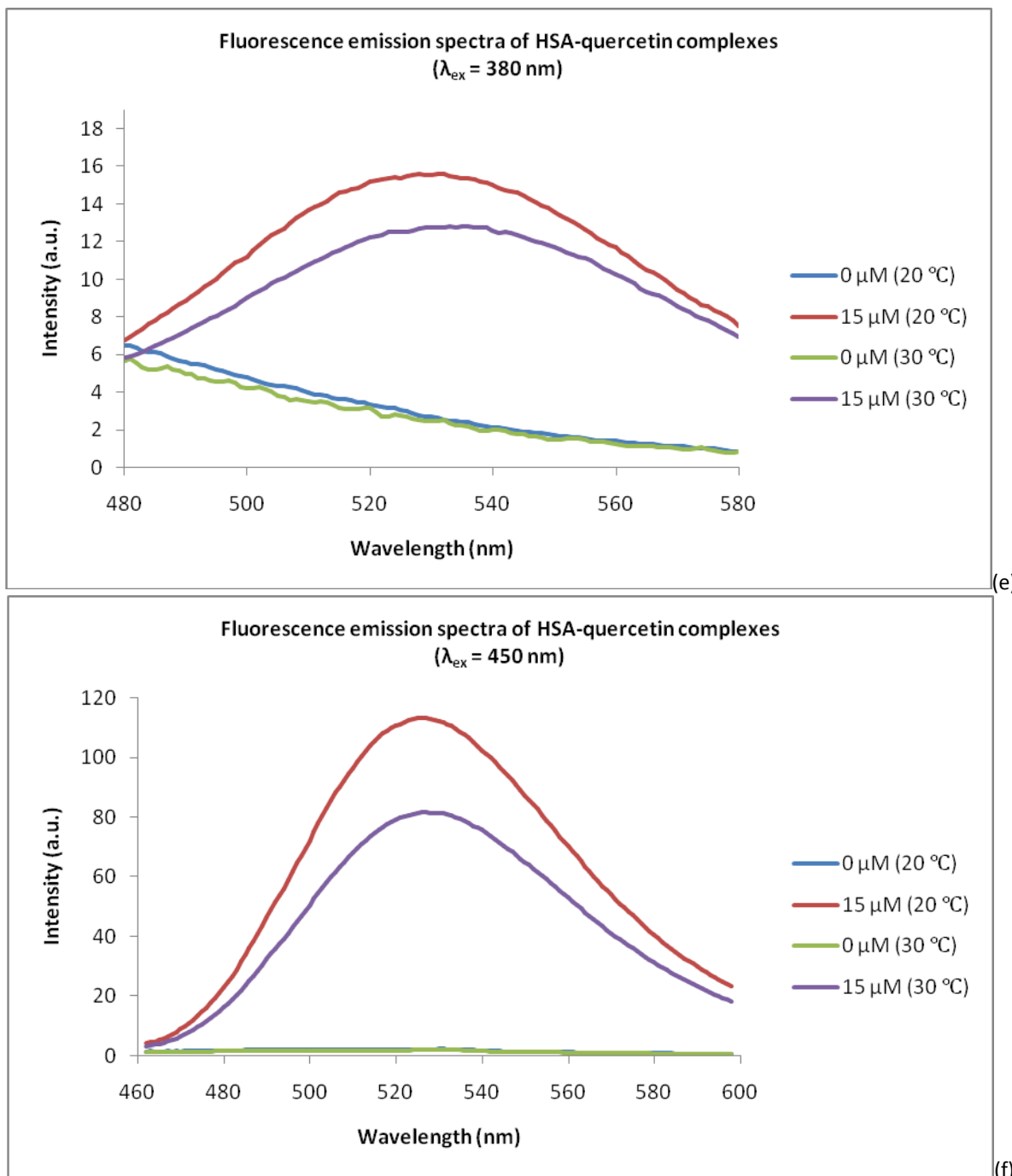
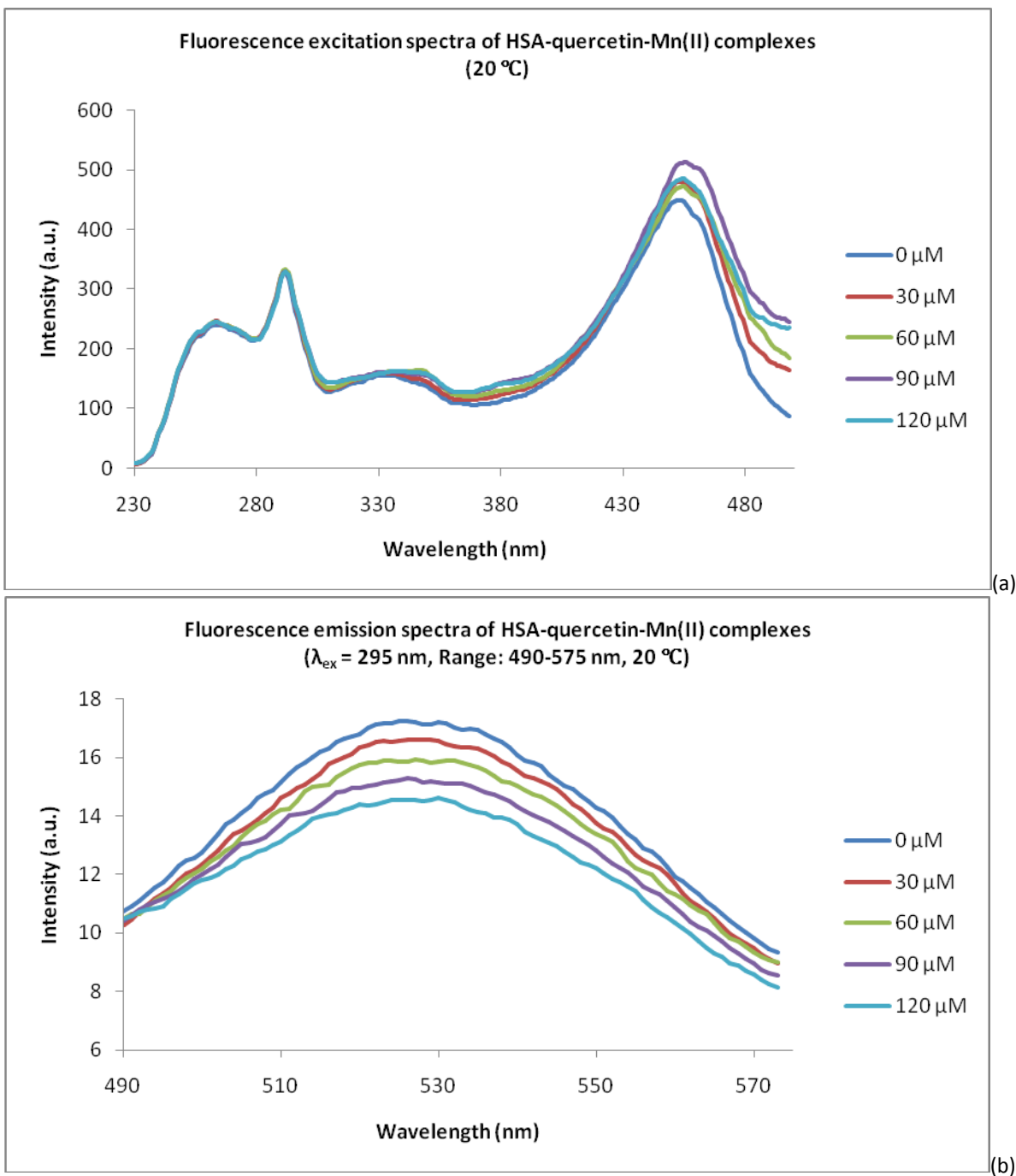
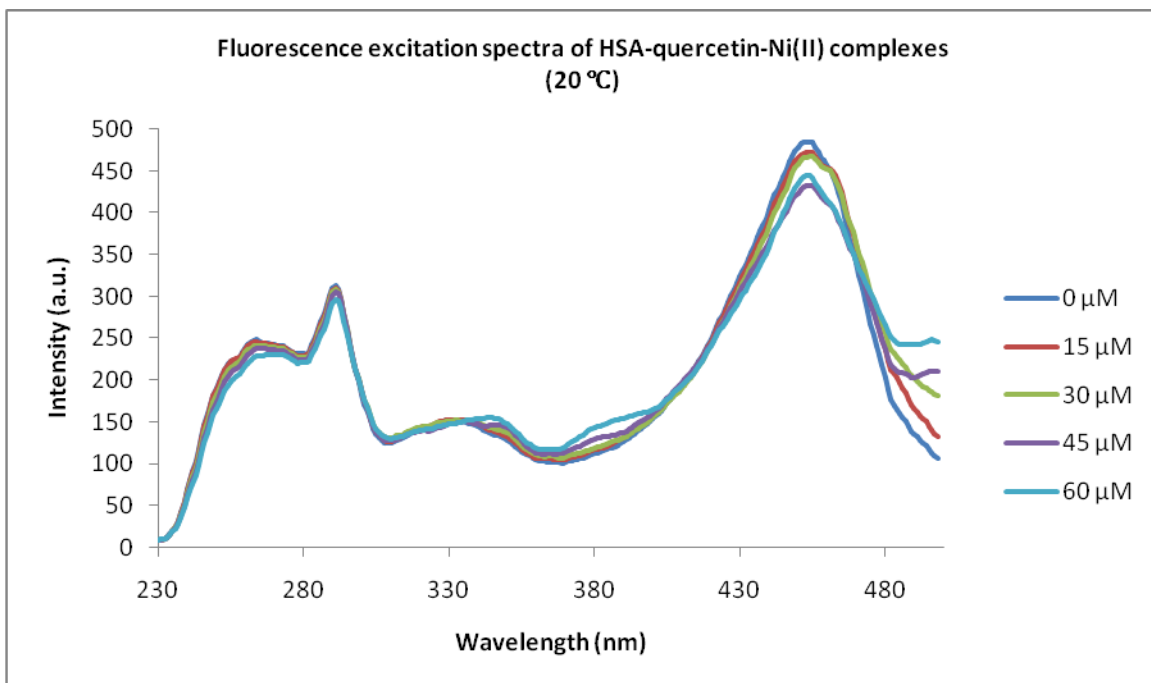


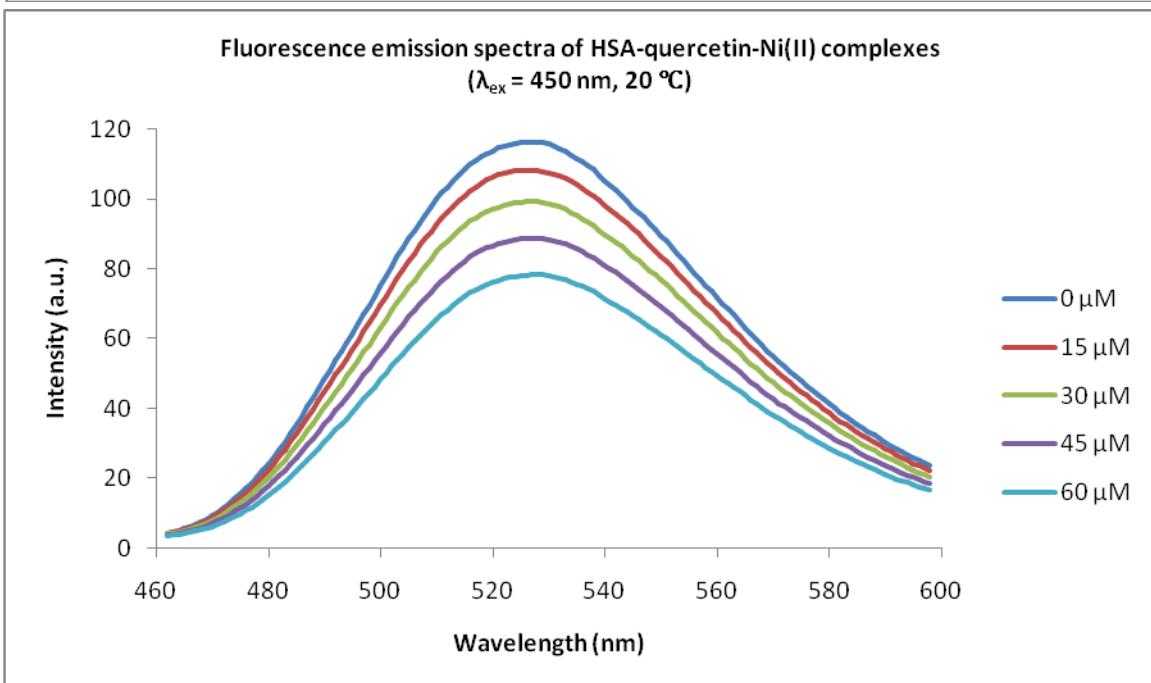
Figure 4: Fluorescence studies of the HSA-querctin complex. All experiments were performed using a 30 μ M HSA solution and a 15 μ M querctin solution in 50 mM Tris-HCl buffer at a temperature of 20 or 30 $^{\circ}$ C, using a scan rate of 120 nm/min (unless otherwise specified). (a) Fluorescence excitation spectra of the HSA-querctin complex (scan rate = 300 nm/min). (b) Fluorescence emission spectra of the HSA-querctin complex ($\lambda_{ex} = 276$ nm). (c) and (d) Fluorescence emission spectra of the HSA-querctin complex ($\lambda_{ex} = 295$ nm). (e) Fluorescence emission spectra of the HSA-querctin complex ($\lambda_{ex} = 380$ nm). (f) Fluorescence emission spectra of the HSA-querctin complex ($\lambda_{ex} = 450$ nm).

Next the effects of divalent metal ions on the HSA-quercetin complex were investigated. As seen in Figure 5a, the HSA-quercetin complex was excited at wavelengths in the range between 230 and 490 nm upon increasing Mn(II) concentration. The addition of Mn(II) does not affect tryptophan or tyrosine excitation. A weakly enhanced excitation near 450 nm is possibly due to transient effects in collisional quenching. Upon increasing temperature, the excitation intensity decreases because the solution viscosity decreases. Resonance energy transfer between a tryptophan residue and quercetin was quenched upon adding Mn(II) (Figure 5b). However, non-fluorescent ground-state formation is also possible since quercetin is known to form a complex structure with Mn(II) [11]. Similarly, changes in excitation around 270 nm indicate that Ni(II) weakly affects the local environment near tyrosine residues (Figure 5c). Furthermore, a decrease in excitation near 450 nm and an increase in excitation near 380 nm indicate that quercetin fluorescence might be altered by Ni(II) addition. Increasing the temperature did not affect the band shape by Ni(II) addition, thus emission spectra are not shown. No band shift due to Ni(II) addition was observed upon exciting quercetin at 450 nm (Figure 5d). The emission of quercetin was clearly quenched in the presence of Ni(II). At 30 °C, the emission spectra were not shifted, but there was quenching of emission peaks due to a decrease in viscosity (Figure 5e). Cu(II) addition into the HSA-quercetin complex results in quenching of fluorescence emission peaks at various excitation wavelengths. This is probably due to very strong affinity of HSA for binding to Cu(II) at the N-terminus. The emission spectra upon excitation at 380 nm are not shown because changes in these spectra show the same patterns as what was observed in emission spectra upon excitation at 295 nm with a range between 490 and 575 nm. Cu(II) addition changed the excitation spectra dramatically, compared to those upon Ni(II) and Mn(II) addition (Figure 5f). Both tryptophan and tyrosine excitation decreased with increasing Cu(II) addition. Furthermore, the excitation at 450 nm shows a band-shift, indicating a change in the quercetin complex structure. In Figure 5g, no significant shift occurs upon increasing temperature compared to the excitation spectra at 20 °C. Excitation intensities in the range between 230 and 490 nm decreased upon increasing the temperature. However, the red-shifted excitation at 450 nm indicates that the HSA-quercetin complex is altered more strongly at higher temperature. A band-shift upon Cu(II) addition is more clearly observed at higher temperatures, as shown in Figure 5h. Therefore, Cu(II) interacts with HSA in a way as to expose tryptophan 214 to the solvent. Increasing the concentration of Cu(II) quenched and very weakly blue-shifted the emission maximum around 530 nm (Figure 5i). The emission spectra obtained by exciting quercetin at 450 nm were not shifted upon Mn(II) and Ni(II) addition. Considering that tyrosine and tryptophan emission were significantly quenched by increasing Cu(II) concentration (see Figure 5h), quenchers binding at the N-terminus of HSA possibly affect the local environment of the HSA-quercetin complex. However, it is not understood why Ni(II) did not shift an emission peak upon excitation at 450 nm, although the degree of band shift was really weak (Figures 5d and 5e). It is possible that no significant band shift occurred because the binding affinity of Ni(II) is significantly weaker than the binding affinity of Cu(II).

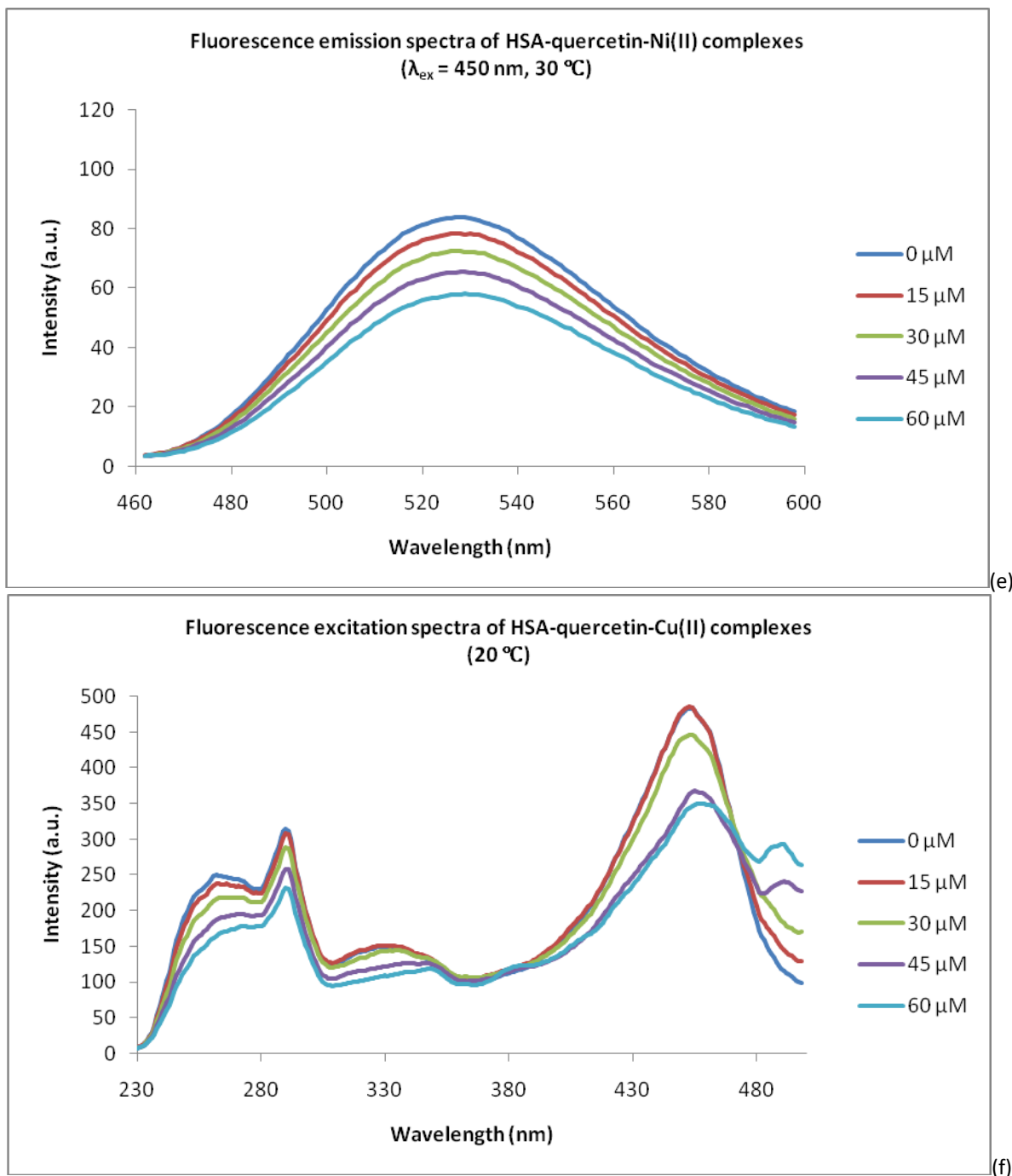


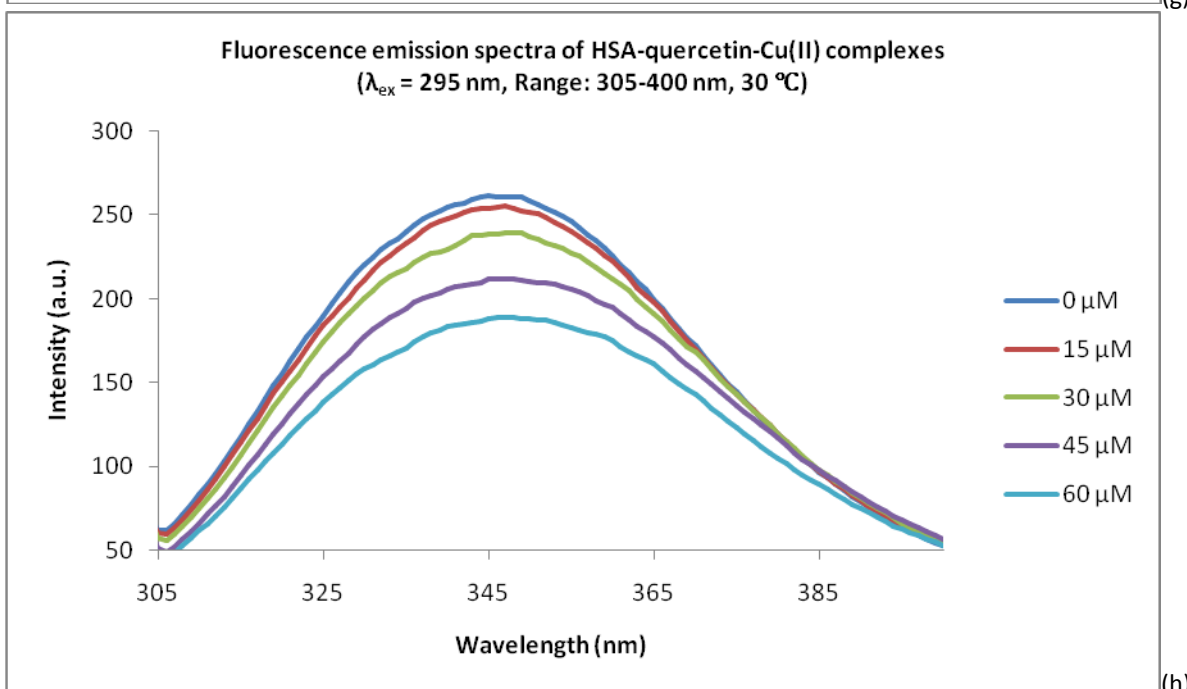
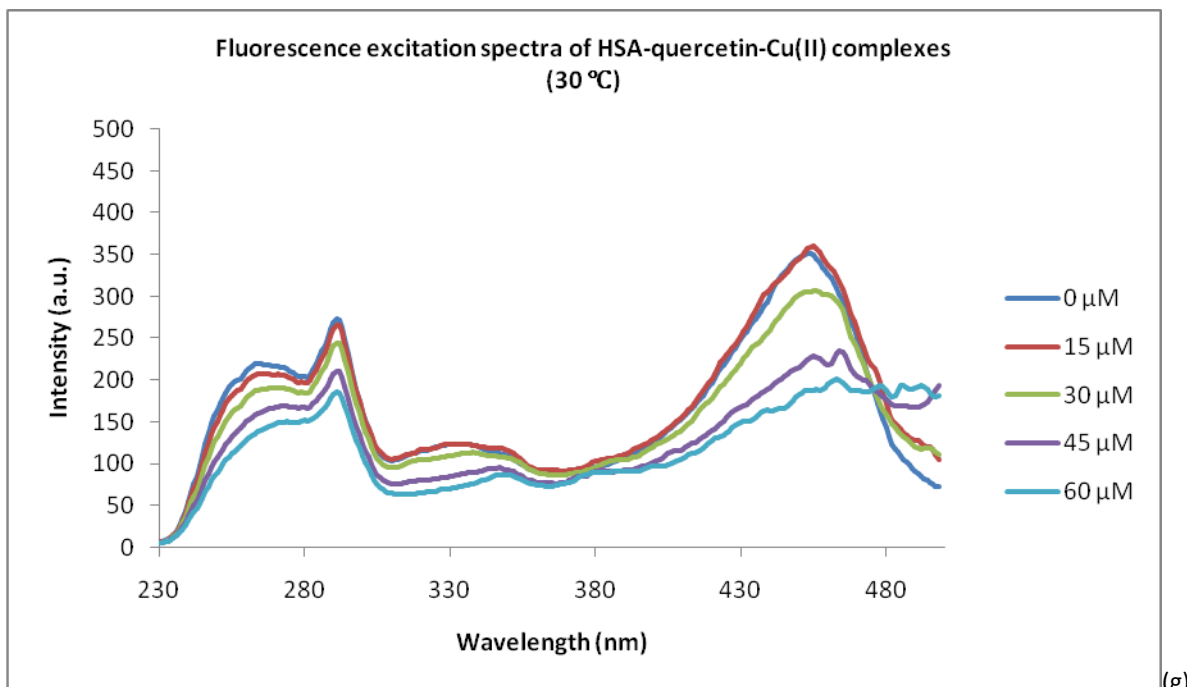


(c)



(d)





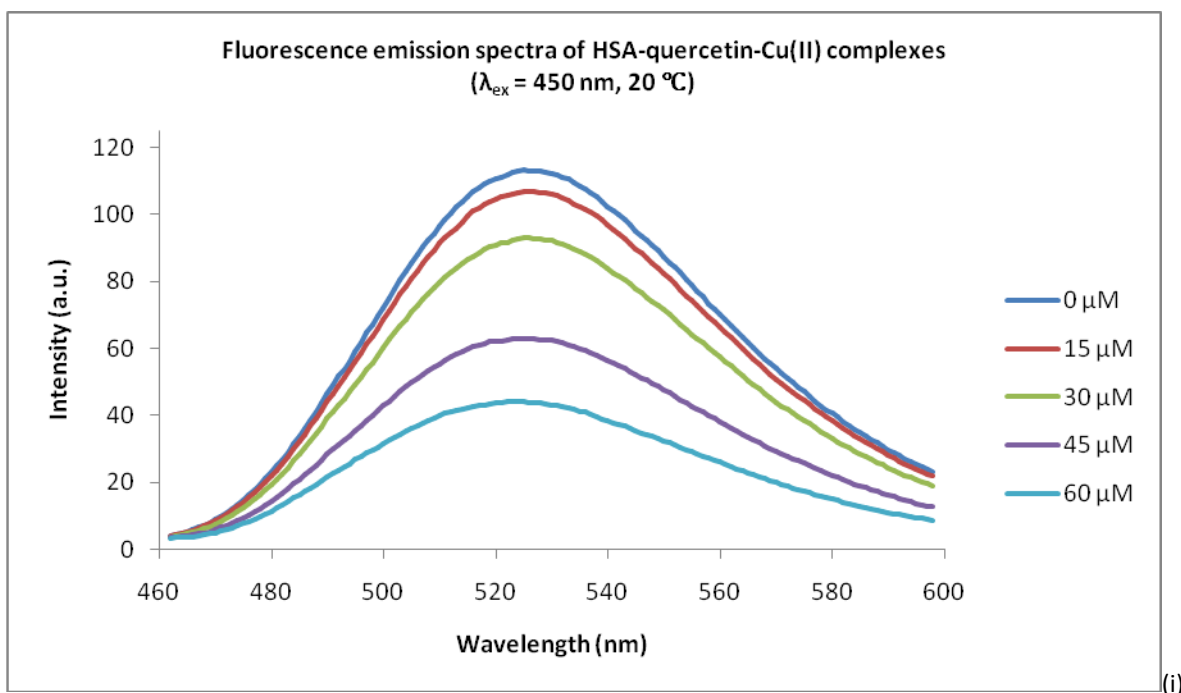
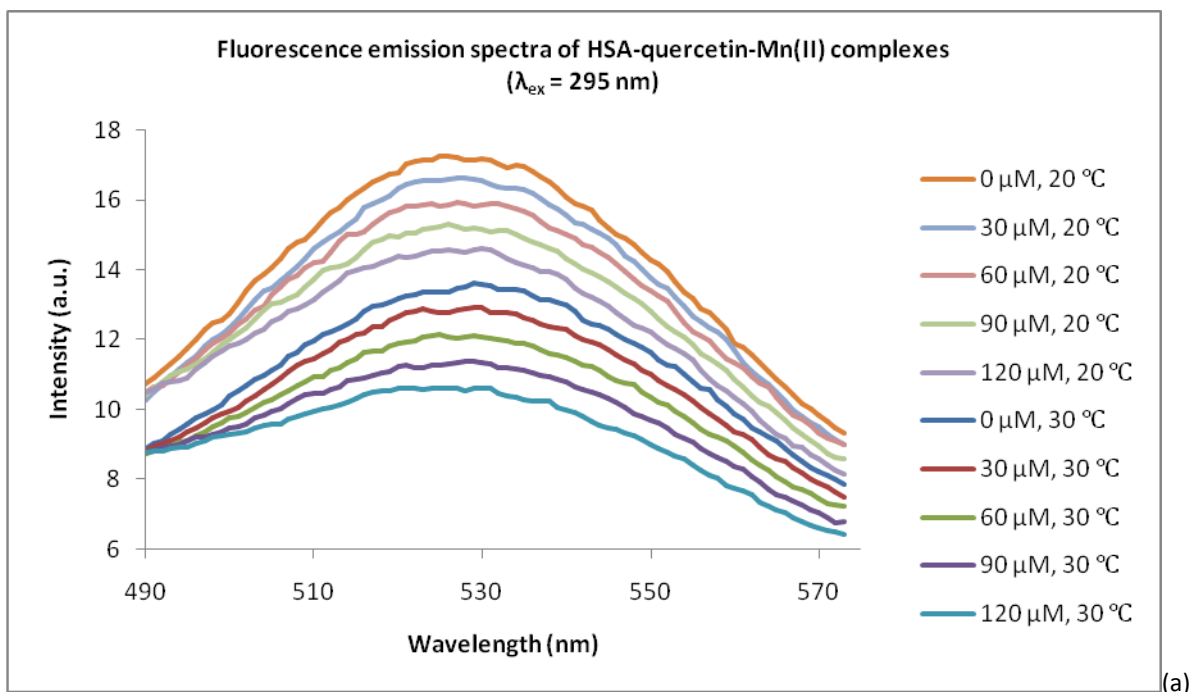
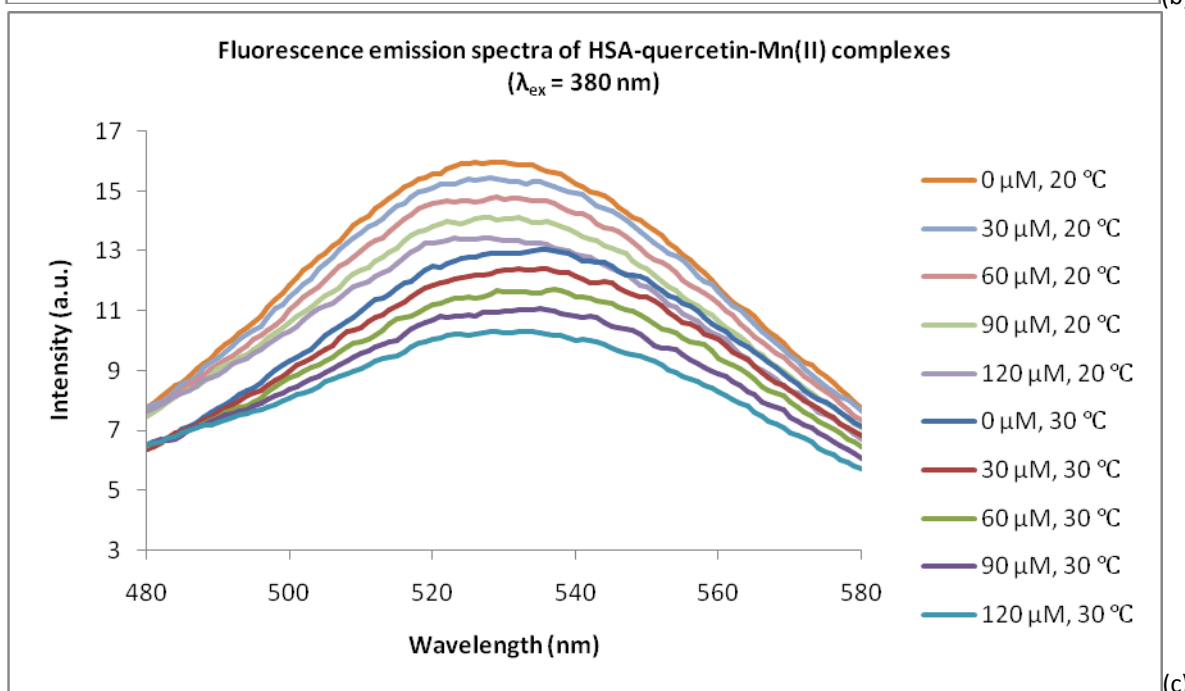
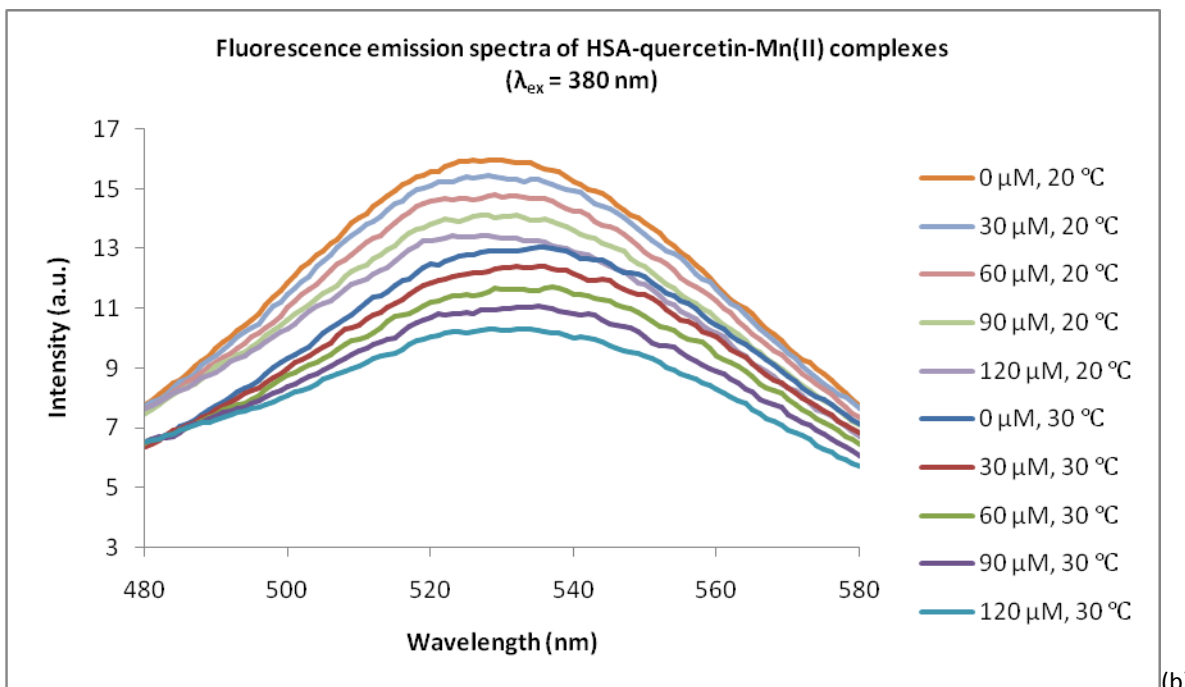


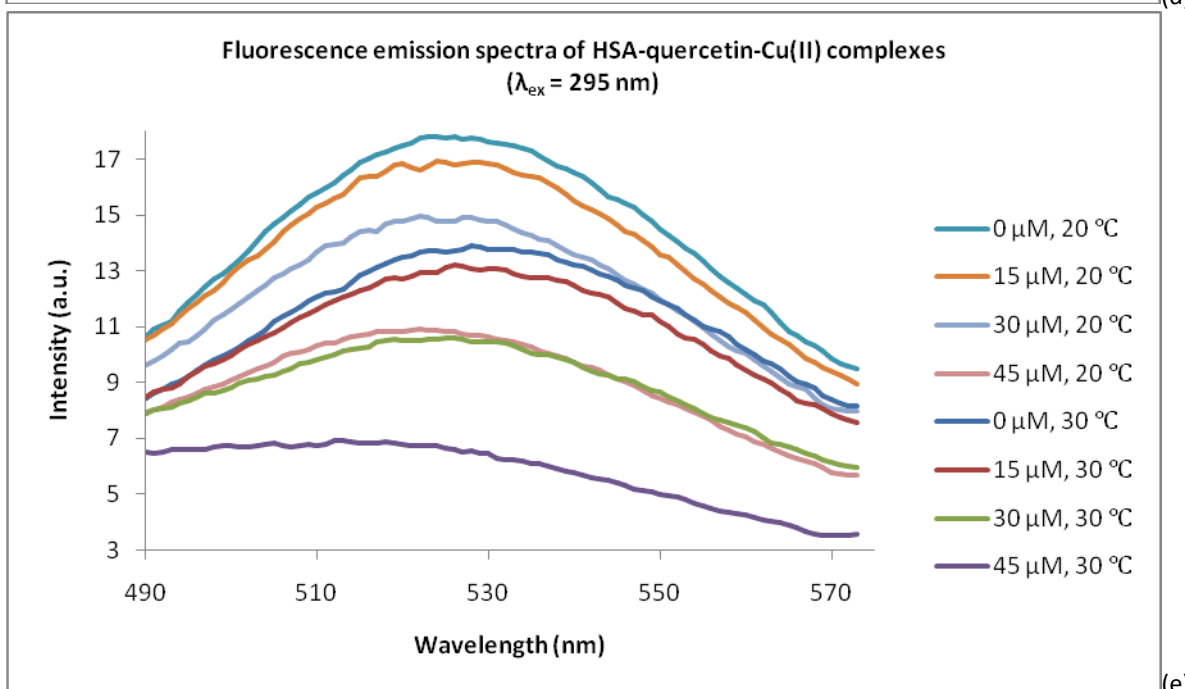
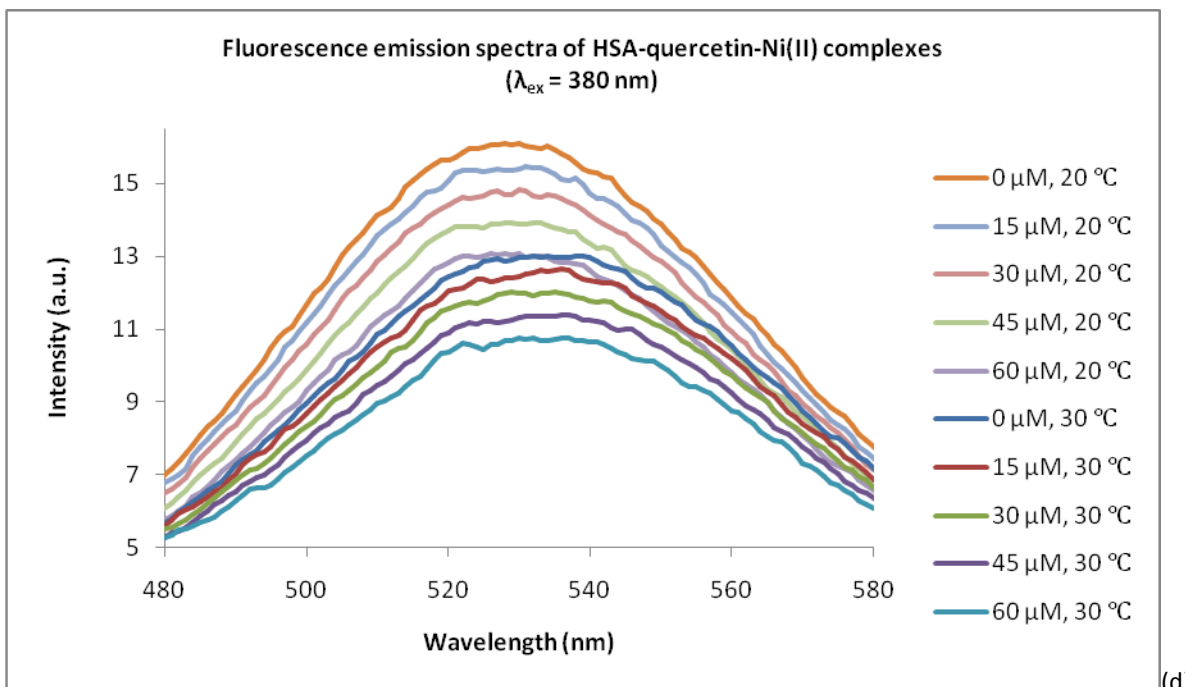
Figure 5: Fluorescence studies of HSA-quercetin-metal ion complexes. All experiments were performed using a scan rate of 120 nm/min, unless otherwise specified. (a) Excitation spectra of solutions containing 30 μM HSA, 15 μM quercetin and varying amounts of Mn(II), in 50 mM Tris-HCl buffer. (b) Emission spectra of the same solutions in (a), using an excitation wavelength of 295 nm. (c) Excitation spectra of solutions containing 30 μM HSA, 15 μM quercetin and varying amounts of Ni(II), in 50 mM Tris-HCl buffer. (d) and (e) Emission spectra of the same solutions in (c), using an excitation wavelength of 450 nm, at temperatures of 20 and 30 $^\circ\text{C}$, respectively. (f) and (g) Excitation spectra of solutions containing 30 μM HSA, 15 μM quercetin and varying amounts of Cu(II), in 50 mM Tris-HCl buffer, at temperatures of 20 and 30 $^\circ\text{C}$, respectively. (h) Emission spectra of the same solutions in (g), using an excitation wavelength of 295 nm. (i) Emission spectra of the same solutions in (f), using an excitation wavelength of 450 nm.

There are a number of characteristics in the fluorescence spectra of the HSA-quercetin-divalent ion system indicating that there are possibly two different quercetin moieties responsible for different excitation. Excitation spectra of the HSA-quercetin complex with three different divalent metals (Figures 5a, 5b, 5f and 5g) show different changes at 290, 380 and 450 nm. When Mn(II) and Ni(II) were added to the HSA-quercetin complex, the excitation intensity at 380 nm increased with increasing concentrations, at both 20 and 30 $^\circ\text{C}$. However, excitation bands at 450 nm exhibited different behavior, decreasing when Mn(II) and Ni(II) were added to the HSA-quercetin complex at 20 $^\circ\text{C}$ but not at 30 $^\circ\text{C}$. From these characteristics, it is quite possible that there are two quercetin moieties excited at different wavelengths. Furthermore, emission maximum bands in the emission spectra of the HSA-quercetin complex with Mn(II), Ni(II) and Cu(II) were shifted to longer wavelengths upon increasing the temperature upon excitation at 295 and 380 nm (Figures 6a-e). However, there were no changes in the band shape of the emission spectra upon excitation at 450 nm when Mn(II) and Ni(II) were added to the HSA-quercetin complex. Furthermore, red-shifted emission bands were observed when Cu(II) was added. It should be stated that the evidence obtained in this study is not adequate to prove the existence of two different quercetin moieties in the HSA-quercetin complex. First,

changes in excitation and emission spectra can be negligible depending on the analysis because emission band shifts are less than 10 nm. Furthermore, when Cu(II) was added to the HSA- quercetin complex, excitation intensities at 380 and 450 nm were decreased except for no change at 380 nm and 20 °C. Nevertheless, two hypothetical quercetin moieties are suggested and labeled as QC1 and QC2. First, QC1 is responsible for the emission around 530 nm upon excitation at 295 and 380 nm. The band shapes of these two emission maxima were very similar. However, it is questionable why this should be the case. Upon excitation, the emergence of fluorescence upon 295 nm was due to resonance energy transfer. This process is non-radiative and does not involve the reabsorption of photons. Thus, it can be assumed that the donor molecule (tryptophan 214) is not affected by the addition of divalent metal ions. However, the acceptor molecule (QC1) may form a complex with, or may be quenched by, metal ions. Then, the tryptophan emission should be enhanced if quercetin emission due to resonance energy transfer decreases since there is a smaller amount of energy transfer. Since tryptophan emission did not change when QC1 emission decreased, it can be assumed that energy transfer still occurred between tryptophan 214 and QC1. However, QC1 in the presence of metal ions is not fluorescent, presumably by forming a ground- or excited-state complex with metal ions. The other part of quercetin in the HSA-quercetin complex that is excited upon a wavelength of 450 nm was designated as QC2. The emission spectra of QC2 upon excitation at 450 nm did not experience a band shift upon temperature change, except when Cu(II) was added.







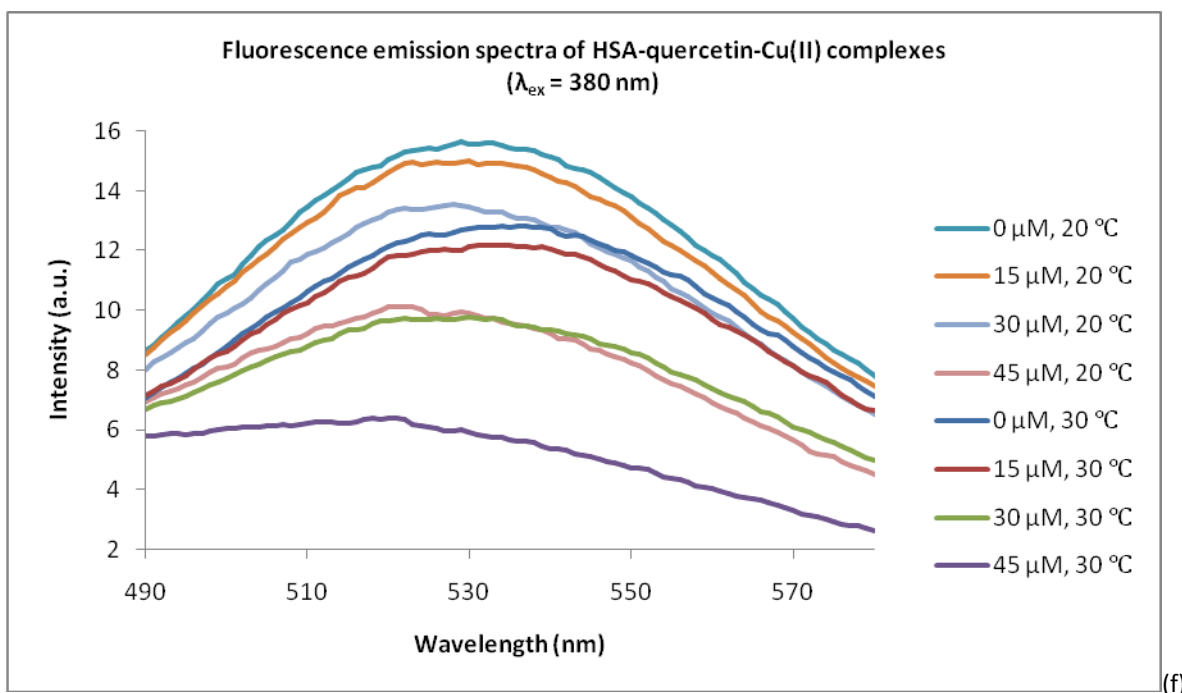


Figure 6: Quercetin fluorescence in HSA-quercetin-metal ion complexes. All emission spectra were recorded using solutions of 30 μ M HSA, 15 μ M quercetin and varying amounts of divalent metal ions, in 50 mM Tris-HCl buffer, at temperatures of either 20 or 30 $^{\circ}$ C (as specified). (a) Emission spectra of Mn(II) complexes using an excitation wavelength of 295 nm (scan rate = 120 nm/min). (b) Emission spectra of Mn(II) complexes using an excitation wavelength of 380 nm (scan rate = 80 nm/min). (c) Emission spectra of Ni(II) complexes using an excitation wavelength of 295 nm (scan rate = 120 nm/min). (d) Emission spectra of Ni(II) complexes using an excitation wavelength of 380 nm (scan rate = 80 nm/min). (e) Emission spectra of Cu(II) complexes using an excitation wavelength of 295 nm (scan rate = 120 nm/min). (f) Emission spectra of Cu(II) complexes using an excitation wavelength of 380 nm (scan rate = 80 nm/min).

A simple, yet powerful, way to interpret quenching is by the use of the Stern-Volmer equation. While mainly considered to express collisional quenching, the Stern-Volmer equation can also be used in static quenching and is written as follows: $\frac{F_0}{F} = 1 + K_{SV}[Q] = 1 + k_q\tau_0[Q]$, where F_0 and F are the fluorescence intensity in the absence and presence of the quencher, respectively; K_{SV} is the Stern-Volmer quenching constant, which in the case of collisional quenching, can be defined as the product of the bimolecular quenching constant (k_q) and the fluorescence lifetime of the unquenched fluorophore (τ_0). The Stern-Volmer equation can be used to determine the mechanism of quenching [9]. A linear relationship indicates that a fluorescent molecule has a single fluorophore, or multiple fluorophores that are all equally accessible by the quencher, and the quenching occurs by collision or complex formation. When the relationship is concave up (toward the y-axis), both collision and complex formation contribute to the quenching of the fluorophore. On the other hand, when the relationship is concave down (toward the x-axis), the quencher has hindered access to the quenching molecule by having different accessibility to two or more populations of the fluorophore in the quenching molecule.

In the case of a linear Stern-Volmer plot, either collision or complex formation can contribute to the quenching. In order to distinguish between these mechanisms, the quenching environment (such as temperature or viscosity) can be varied, or the fluorescence lifetime could be used [10]. Upon increasing temperature, molecules diffuse faster and hence larger amounts of collisional quenching occurs. The fluorescence intensity in the presence of the quencher decreases, therefore the relative fluorescence increases. As a result, the Stern-Volmer plot shifts toward the x-axis as an effect of increasing temperature. However, if a complex is formed by the fluorescence molecule and the quencher it can be dissociated (if it is weakly bound) by increasing temperature, hence there are smaller amounts of static quenching. Therefore the Stern-Volmer plot shifts toward the y-axis.

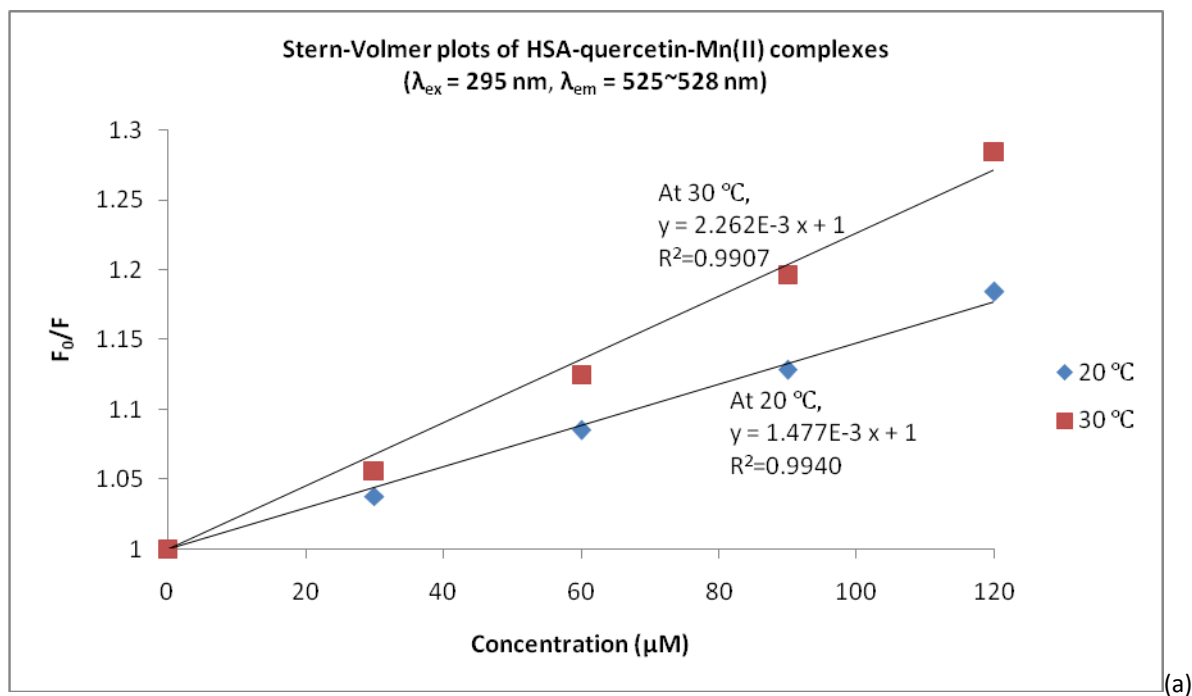
A best-fit line and corresponding R^2 value were calculated for each Stern-Volmer plot when applicable. When R^2 values are low (< 0.99), the relationship is not considered to be linear. A number of emission spectra having a very weak band shift in this study were included to generate the Stern-Volmer plots. Furthermore, noise around the emission peaks was observed in nearly all cases. Therefore, the average of F_0/F was taken by considering both band shift and noise.

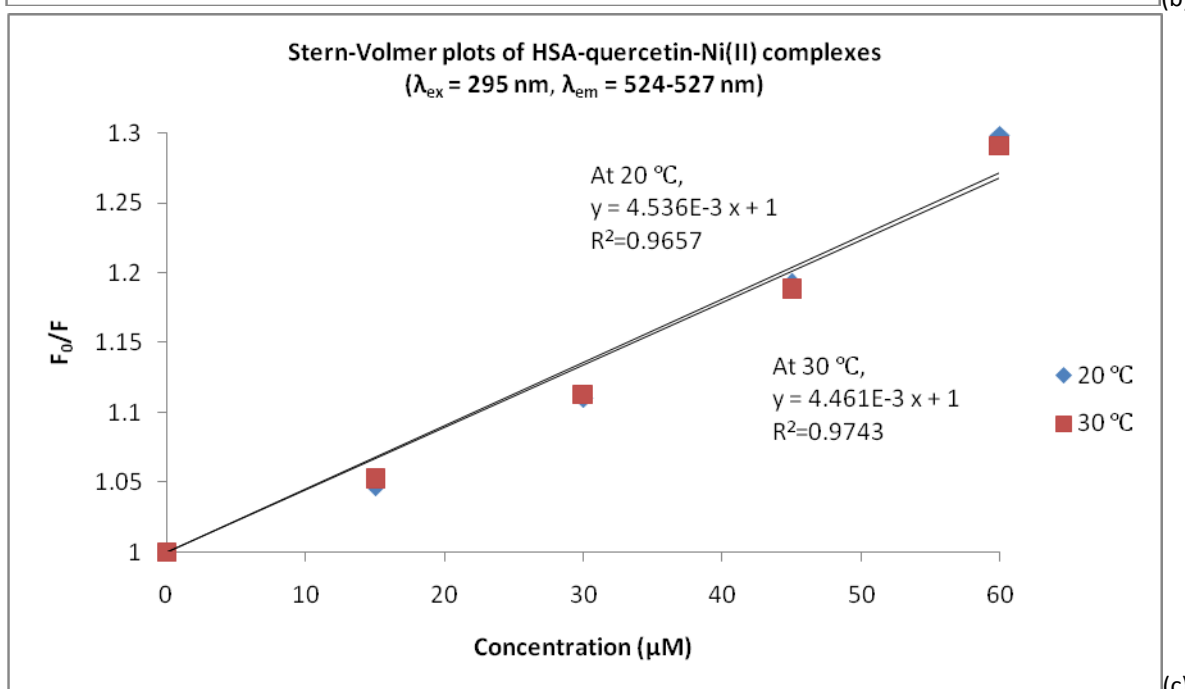
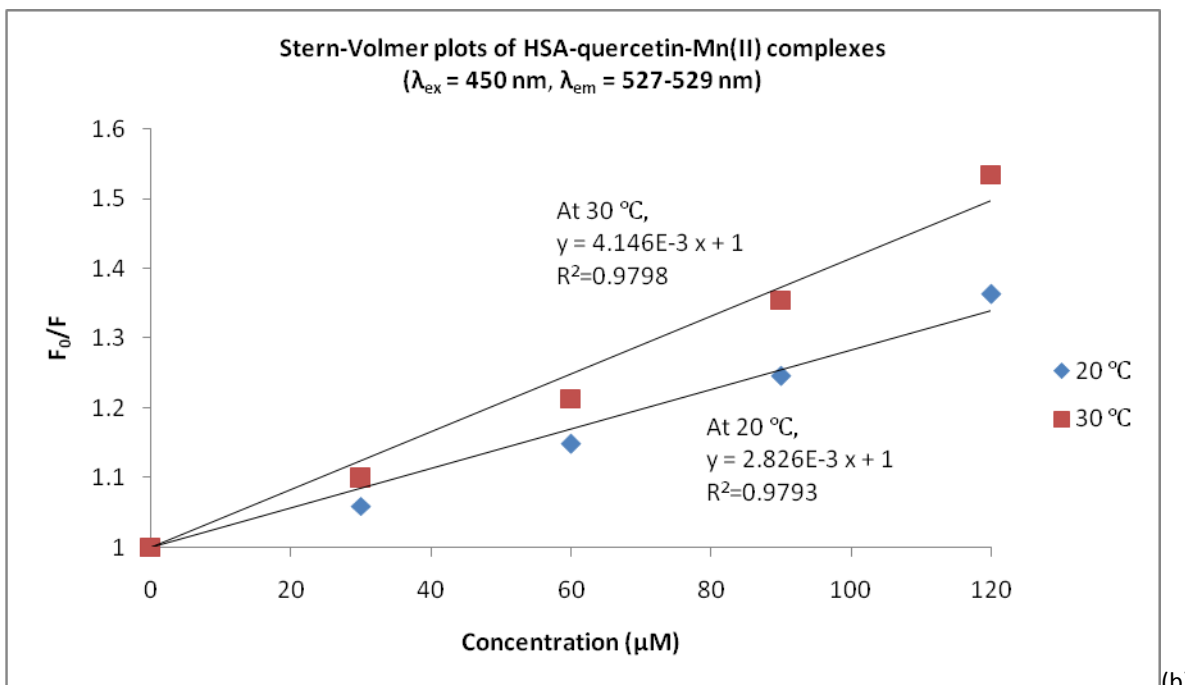
QC1 was excited by a tryptophan emission due to an excitation at 295 nm and emitted a peak of maximum intensity around 526 nm. Using the linear relationships calculated with the Stern-Volmer plots in Figure 7a, the K_{SV} values at 20 and 30 °C are 1.477×10^3 and 2.262×10^3 L/mol, respectively. The average of two emission maximum wavelengths (525 and 526 nm) was used for each data point due to the noise around emission peaks at different quencher concentrations. The emission maximum intensity for each quencher concentration was shifted to longer wavelengths and found at 528 nm. R^2 values for each slope are very close to 1, indicating a linear relationship at each temperature. Since the Stern-Volmer plot shifts toward the y-axis at higher temperatures, it is more likely that quenching of the quercetin complex by Mn(II) is due to collision. Upon an excitation at 450 nm, a maximum emission by QC2 was observed around 528 nm. Here, the corresponding K_{SV} 's are calculated to be 2.826×10^3 and 4.416×10^3 L/mol, respectively (Figure 7b). Collisional quenching is the dominant mechanism; however a decrease in the R^2 values indicates that other quenching mechanisms may make minor contributions. Experimental errors were very unlikely to be the reason for the decrease in the R^2 values since the two data sets have regressions whose correlation coefficients are very close to each other.

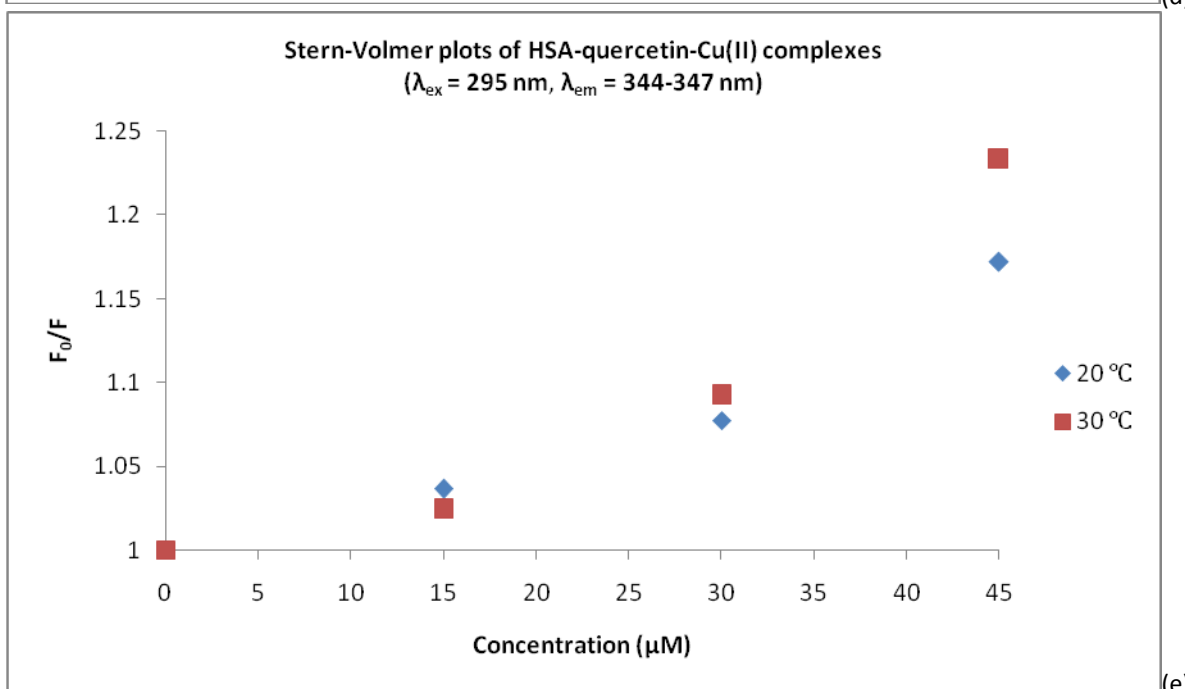
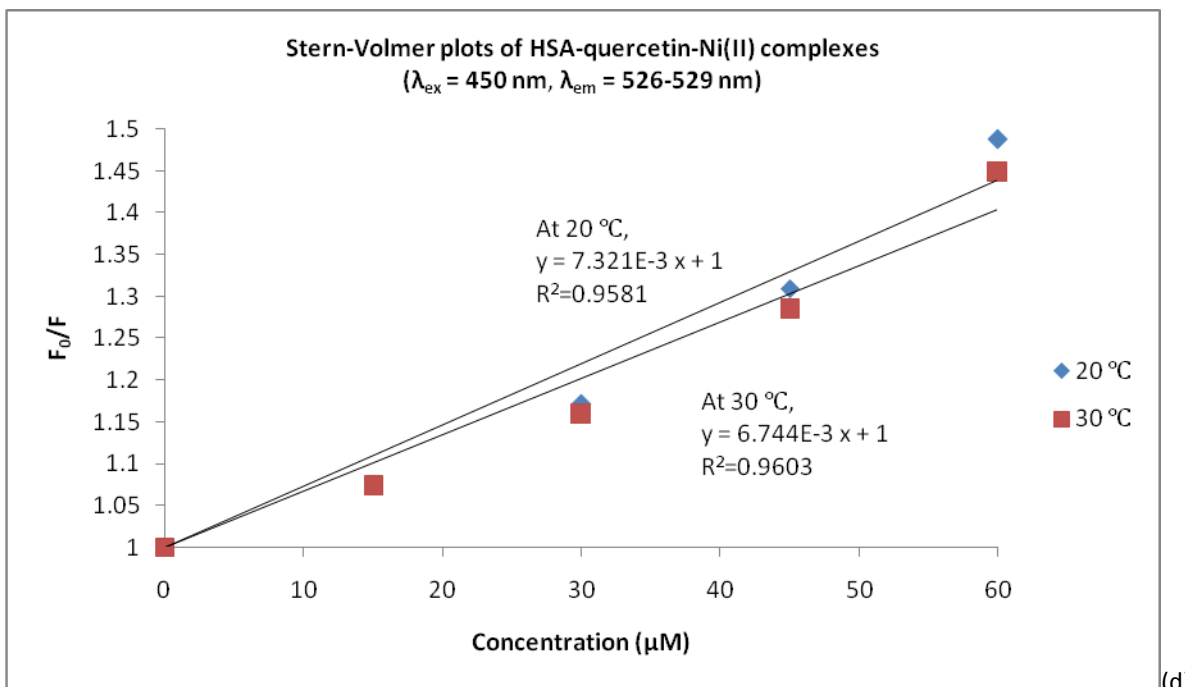
For Ni(II), the quenching mechanism could not be determined since increasing the temperature did not cause a different slope in the Stern-Volmer plot at 20 °C vs. 30 °C (Figures 7c and 7d). Because of the relatively low R^2 values, a linear relationship was not clearly established for either temperature using either excitation wavelength. However, ground-state complex formation is likely to be more significant in quenching QC2 emission since the values of F_0/F move towards the x-axis upon an increase in temperature.

In the case of adding Cu(II) in solutions containing the HSA-quercetin complex, a quencher addition shifted the emission maximum significantly. Both static and collisional

quenching are responsible for the decrease in the emission peak around 345 nm upon excitation at 295 nm since the Stern-Volmer plots clearly have a non-linear relationship deviating toward the y-axis (Figure 7e). A change in the degree of band shift due to temperature change was not clearly observed in this case. However, a band shift of emission peaks due to increasing the quencher concentration was clearly present (Figure 5h). Therefore, a broad range of emission maximum wavelengths was used in order to generate the Stern-Volmer plot. The quenching mechanism dominant at low concentrations of Cu(II) is possibly static quenching since F_0/F decreases upon increasing the temperature. However, collisional quenching is dominant in solutions having Cu(II) concentrations greater than 30 mM. Figures 7f and 7g also show a non-linear relationship at their respective excitation wavelengths. Therefore, the quenching mechanism due to Cu(II) addition is due to both collision and ground-state complex formation. However, it is still observable that collisional quenching is dominant considering that F_0/F increases upon increasing temperature.







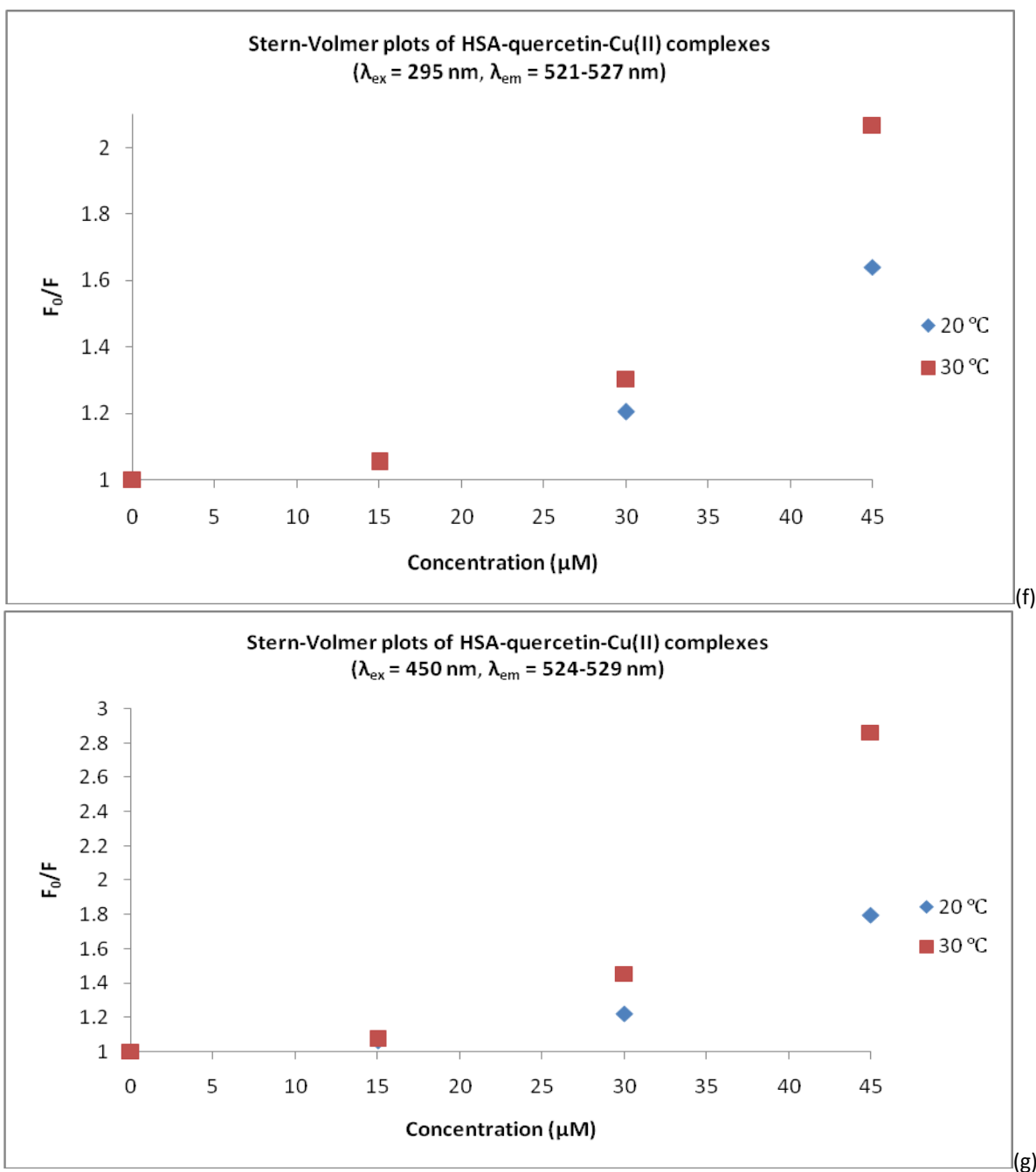


Figure 7: Stern-Volmer plots to determine the quenching mechanism(s) in HSA-quercetin-metal ion complexes. All emission spectra were recorded using solutions of 30 μM HSA, 15 μM quercetin and varying amounts of divalent metal ions, in 50 mM Tris-HCl buffer, at temperatures of either 20 or 30 °C (as specified). (a) Analysis for Mn(II) using an excitation wavelength of 295 nm and emission wavelengths between 525-528 nm. (b) Analysis for Mn(II) using an excitation wavelength of 450 nm and emission wavelengths between 527-529 nm. (c) Analysis for Ni(II) using an excitation wavelength of 295 nm and emission wavelengths between 524-527 nm. (d) Analysis for Ni(II) using an excitation wavelength of 450 nm and emission wavelengths between 526-529 nm. (e) Analysis for Cu(II) using an excitation wavelength of 295 nm and emission wavelengths between 344-347 nm. (f) Analysis for Cu(II) using an excitation wavelength of 295 nm and emission wavelengths between 521-527 nm. (g) Analysis for Cu(II) using an excitation wavelength of 450 nm and emission wavelengths between 524-529 nm.

CONCLUSIONS

HSA-quercetin complexes in the presence of Cu(II), Ni(II) or Mn(II) were studied using fluorescence spectroscopy. Before performing the binding studies, changes in fluorescence spectra due to unwanted factors had to be checked. First, the solvent effect was considered to potentially change fluorescence excitation and emission by changing the local environment of the fluorophore. Even though the experiment was designed to add solvents in an amount less than 1% of the total volume, a change in fluorescence excitation and emission was carefully monitored, showing that the solvent effect was negligible. Additional experiments were also performed by recording fluorescence spectra of Cu(II), Ni(II) or Mn(II) in 50 mMTris-HCl buffer, supporting the interpretation of spectra recorded in the presence of the HSA-quercetin complex with quenching metal ions. Finally, experiments were done by adding 15 mMquercetin to HSA in order to determine fluorescence quenching and band shifts due to quercetin. After performing preliminary experiments and researching previous studies, the parameters shown in Table 1 were obtained.

Table 1: Excitation and emission wavelengths used for recording fluorescence spectra.

λ_{ex} (nm)	λ_{em}^* (nm)	Excitation Target
276	340	Tryptophan and tyrosine residues
295	345	Tryptophan-214
295	525	QC1 by resonance transfer
380	525	QC1
450	525	QC2

*The emission peaks fluctuated within a small range of wavelengths depending on the shift or noise

Emission wavelengths were shifted to shorter or longer wavelengths by adding a quencher, and the degree of the shift depended on the quencher type. Upon an excitation at 295 nm, fluorescence resonance energy was transferred by tryptophan-214 emission to QC1. QC1 was excited in the same manner upon an excitation at 295 or 380 nm. Another possible quercetin moiety in the complex structure was QC2, which was sensitive to an excitation at 450 nm. The two different quercetin moieties within the HSA-quercetin complex, QC1 and QC2, could be distinguished by changing the temperature. While the emission spectrum of QC2 was not quenched and insignificantly blue-shifted upon increasing temperature from 20 to 30 °C, QC1 was quenched and shifted to longer wavelengths.

Fluorescence quenching studies of the HSA-quercetin complex by Cu(II), Ni(II) and Mn(II) were performed by interpreting fluorescence spectra using the corresponding Stern-Volmer plots. The quenching and band-shift upon addition of various quenchers to the HSA-quercetin complex are summarized in Tables 2-4. As the temperature increased, emission peaks were quenched in all emission spectra. An excitation at 276 nm in the HSA-quercetin-metal ion complex results in broad emission peaks by tryptophan and tyrosine residues. A change in the peaks around 340 nm after Mn(II) and Ni(II) addition was insignificant, including the negligible effect by Ni(II) on energy transfer between tryptophan and tyrosine residues. Only tryptophan-

214 was able to be excited at 295 nm without exciting tyrosine residues. Once again, a change in tryptophan emission by Mn(II) and Ni(II) addition was insignificant because the degree of change in intensity was small. Therefore, Mn(II) and Ni(II) do not affect tryptophan and tyrosine residues when HSA forms a complex with quercetin. However, Cu(II) was still able to quench tryptophan and tyrosine fluorescence due to its strong binding affinity to HSA.

Table 2: Summary of fluorescence emission spectra of the HSA-quercetin complex upon the addition of Mn(II).

Spectral Classification	λ_{ex} (nm)	λ_{em}^* (nm)	Temp. (°C)	Quencher Effect	Temperature Effect***
$Em_{trp,tyr}$	276	339-340	20	enhances a peak**	quenches a peak
		337-338	30	enhances a peak**	
Em_{trp}	295	345-346	20	enhances a peak**	quenches a peak
		344-347	30	enhances a peak**	
$Em_{QC1,295}$	295	525-526	20	quenches a peak	quenches a peak, red-shifted band
		528	30	quenches a peak	
$Em_{QC1,380}$	380	528-529	20	quenches a peak	quenches a peak, red-shifted band
		531-536	30	quenches a peak	
Em_{QC2}	450	527-528	20	quenches a peak	quenches a peak
		528-529	30	quenches a peak	

*The emission peaks fluctuated within a small range of wavelengths depending on the shift or noise. **The change is small and can be considered negligible. *** The effect was observed by superimposing emission spectra recorded at 20 and 30 °C

Table 3: Summary of fluorescence emission spectra of the HSA-quercetin complex upon the addition of Ni(II).

Spectral Classification	λ_{ex} (nm)	λ_{em}^* (nm)	Temp. (°C)	Quencher Effect	Temperature Effect***
$Em_{trp,tyr}$	276	338-339	20	quenches a peak (~310 nm)**, enhance a peak (~340 nm)**	quenches a peak
		337-338	30	quenches a peak (~310 nm)**, enhance a peak (~340 nm)**	
Em_{trp}	295	344-348	20	Noise****	quenches a peak
		344-346	30	quenches a peak**	
$Em_{QC1,295}$	295	524-525	20	quenches a peak	quenches a peak, red-shifted band
		526-527	30	quenches a peak	
$Em_{QC1,380}$	380	527-528	20	quenches a peak	quenches a peak, red-shifted band
		533-536	30	quenches a peak	
Em_{QC2}	450	526-527	20	quenches a peak	quenches a peak
		527-529	30	quenches a peak	

*The emission peaks fluctuated within a small range of wavelengths depending on the shift or noise. **The change was small and can be considered negligible. ***The effect was observed by superimposing emission spectra recorded at 20 and 30 °C. ****The change was observed without a distinct pattern.

Table 4: Summary of fluorescence emission spectra of the HSA-quercetin complex upon the addition of Cu(II).

Spectral Classification	λ_{ex} (nm)	λ_{em}^* (nm)	Temp. (°C)	Quencher Effect	Temperature Effect***
$Em_{trp,tyr}$	276	339-341	20	quenches a peak	quenches a peak
		337-338	30	quenches a peak	
Em_{trp}	295	345-347	20	weak red-shifted band**, quenches a peak	quenches a peak
		344-346	30	weak red-shifted band**, quenches a peak	
$Em_{QC1,295}$		524-526	20	blue-shifted band, quenches a peak	quenches a peak, red-shifted band
		521-527	30	blue-shifted band, quenches a peak	
$Em_{QC1,380}$	380	521-528	20	blue-shifted band, quenches a peak	quenches a peak, red-shifted band
		527-532	30	blue-shifted band, quenches a peak	
Em_{QC2}	450	524-526	20	weak blue-shifted band**, quenches a peak	quenches a peak
		525-529	30	weak blue-shifted band**, quenches a peak	

*The emission peaks fluctuated within a small range of wavelengths depending on the shift or noise. **The change was small and can be considered negligible. ***The effect was observed by superimposing emission spectra recorded at 20 and 30 °C.

Emission peaks near 530 nm upon excitation at 295 and 380 nm shared spectral changes. In the case of Ni(II) and Mn(II) addition, both $Em_{QC1,290}$ and $Em_{QC1,380}$ showed a weak red-shifted band upon an increase of temperature. When Cu(II) was added to the HSA-quercetin complex, emission bands were shifted to longer wavelengths moderately as the temperature increased. However, the emission band in Em_{QC2} in the presence of Ni(II) and Mn(II) was not shifted upon increasing temperature, while the addition of Cu(II) caused a weak blue-shifted emission maximum. Therefore, it is possible that QC1 and QC2 are actually different quercetin moieties in the HSA-quercetin complex.

In the emission spectra with Cu(II) and Mn(II) addition upon excitations at 295 and 380 nm (Figures 6a, b, d and e), emission bands are clearly shifted to longer wavelengths. However, in the case of Ni(II) addition, the band shift does not occur as strongly. This can be related to the Stern-Volmer plots of Ni(II) emission peaks having ambiguous changes due to changing the temperature. The QC2 emission peaks were not shifted by the temperature except in the case when Cu(II) was added to the HSA-quercetin complex.

It should be stated that the data presented in Figures 6 and 7 is not adequate to prove the existence of QC1 and QC2 in the HSA-quercetin complex. Even though QC1 emission shifts were noticeable in the case of Mn(II) and Cu(II) addition, the change in wavelength due to the temperature change was less than 10 nm in the case of Ni(II). When Ni(II) was added to the HSA-quercetin, increasing the temperature by 10 °C only shifted the emission maximum by 2 nm. Furthermore, increasing the temperature in the HSA-quercetin-Cu(II) complexes even shifted the QC2 emission peak. Therefore, further experiments are necessary in order to prove

the assumption that there are two quercetin moieties excited by different excitation wavelengths.

Table 5: Summary of the Stern-Volmer constants for HSA-quercetin complexes quenched by divalent metal ions.

Quencher Type	Spectral Classification	Temp. (°C)	K_{SV} ($10^3 L/mol$)	Direction of the SV Plot Moving upon Increasing Temperature
Mn(II)	$Em_{QC1,295}$	20	2.262	y-axis
		30	1.477	
	Em_{Q2}	20	2.826	y-axis
		30	4.146	
Ni(II)	$Em_{QC1,295}$	20	4.536	x-axis*
		30	4.461	
	Em_{Q2}	20	7.321	x-axis
		30	6.744	
Cu(II)	$Em_{QC1,295}$	20	N/A	N/A
		30		
	Em_{Q2}	20		y-axis
		30		
	Em_{trp}	20		y-axis
		30		

*The change is small and can be considered negligible

The Stern-Volmer plots at 20 and 30 °C for quenching the HSA-quercetin complex by Mn(II), Ni(II) and Cu(II) are summarized in Table 5. Only the Stern-Volmer relationships having high R^2 values for the regression were used to determine the quenching mechanism. A linear Stern-Volmer relationship was only observed in the case of QC1 quenching by Mn(II). Other Stern-Volmer plots, including QC1 and QC2 quenching by Cu(II) and Ni(II) and QC2 quenching by Mn(II), resulted in R^2 values less than 0.99, implying a non-linear relationship. When a non-linear relationship was observed, the Stern-Volmer plot had an upward curvature and was concave towards the y-axis, with the degree of concavity depending on the quencher type. A non-linear Stern-Volmer relationship indicates a combination of collisional and static quenching. When the data in a Stern-Volmer plot shift towards the y-axis or x-axis by increasing the temperature, the quenching can be attributed to collisional or static quenching, respectively. In the case of the observed Stern-Volmer plot, which was concave up and toward the y-axis, a combination of two quenching mechanisms was suspected. However, the temperature dependence was still investigated in order to determine which quenching mechanism would be dominant. From Table 5, QC1 was quenched by collisions in the presence of Mn(II). However, both collisional and static quenching occurred when QC2 was quenched, with the major contribution coming from collisional quenching. On the other hand, the ground-state complex formation by the quercetin moiety in the HSA-quercetin complex with addition of Ni(II) was expected since the concave Stern-Volmer plots moved toward the x-axis. However, the temperature change in the case of Ni(II) quenching QC1 barely affected the Stern-Volmer slope. When Cu(II) was added to the HSA-quercetin complex, a non-linear Stern-Volmer relationship was noticeable in all cases, therefore the Stern-Volmer constant and R^2 values

were not calculated. However, the quenching was possibly accomplished mainly by collisions, as judged from the change in the Stern-Volmer plots by varying the temperature.

In conclusion, two fluorescence quercetin moieties (QC1 and QC2) in the HSA-quercetin complex possibly exist and are excited upon different wavelengths. QC1 was found to be excited by resonance energy transfer upon tryptophan emission at 295 nm and is highly sensitive to both temperature change and quencher addition. Emission spectra upon excitation at 380 nm were compared with emission spectra upon excitation at 295 nm, showing these two excitations eventually targeted the same moiety. Without the quenching molecule, the emission maxima of QC1 and QC2 were approximately 15 and 100 a.u., respectively. QC2 was only sensitive to Cu(II) addition, indicating that the emission by QC2 would be strongly related to the protein structure since Cu(II) quenches both tryptophan and tyrosine residues. Fluorescence spectra changes upon varying the temperature would be due to change in the local environment of the fluorophore. Therefore, it is assumed that the relatively buried QC2 was able to withstand the temperature change while the relatively exposed QC1 was more affected. However, both QC1 and QC2 are within the same structure; therefore they are quenched in the same manner. It was quite interesting that Ni(II) and Cu(II) showed different quenching mechanisms for QC1 and QC2. Even though the quenching was done by both collisional and static quenching in the presence of Ni(II) and Cu(II), QC1 and QC2 were quenched more by the ground-state complex formation by Ni(II), while collisional quenching was dominant in the case of Cu(II) quenching. Additionally, divalent metal ion quenching of the HSA-quercetin complex was also affected by the degree of metal ion binding affinity to HSA. Cu(II), strongly binding to HSA, showed a strong quenching behavior and caused an emission band shift on QC1 and QC2, while Ni(II) and Mn(II) did not quench QC1 and QC2 as strongly. This is particularly true for Mn(II), having the weakest binding affinity among the three metal ions used, which quenched QC1 and QC2 weakly. Therefore, it was also possible that the binding of metal ions to HSA also affected QC1 and QC2 quenching. In summary, two extrinsic fluorophores were observed to form ground-state complexes with HSA and quercetin, and they are quenched by divalent metal ions. The quenching was usually contributed to by both collisional and static quenching. The quencher type affected the degree of quenching and the emission band shape. However, any correlation with the quencher characteristics, such as the binding affinity and binding sites on HSA, was not found in these experiments.

ACKNOWLEDGMENTS

We would like to thank Victoria Heinz and Patrick Chiu for their assistance with this project.

REFERENCES

- [1] Bertini I, Sigel A, Sigel H. Handbook of Metalloproteins, Marcel Dekker, New York 2001; 858-863.
- [2] Sugio S, Kashima A, Mochizuki S, Noda M, Kobayashi K. Protein Engineering 1999; 12: 439-446.



- [3] Peters T. Jr All About Albumin: Biochemistry, Genetics and Medical Applications 1st ed Elsevier Missouri 1995.
- [4] Sadler PJ, Viles JH. Inorg Chem 1996; 35: 4490-4496.
- [5] Silvio A, Simonetta C, Simonetta GC, Enzo T. Magn Reson Chem 2002; 40: 41-48.
- [6] Torreggiani A, Tamba M, Trincherro A, Bonora S. J Mol Struct 2005; 744-747: 759-766.
- [7] Formica JV, Regelson W. Fd Chem Toxic 1995; 33(12): 1061-1080.
- [8] Skoog DA, Holler FJ, Crouch SR. Principles of Instrumental Analysis. Thomson, California, 2007; 6: 399-412.
- [9] Vivian JT, Callis PR. Biophys J 2001; 80: 2093-2109.
- [10] Lakowicz JR. Principles of Fluorescence Spectroscopy. Springer New York, 2006; 3.
- [11] Zhou J, Wang L, Wang J, Tang N. Transition Met Chem 2001; 26: 57-63.
- [12] Brown JE, Khodr H, Hider RC, Rice-Evancs A. Biochem J 1998; 330: 1173-1178.
- [13] Mira L, Fernandez MT, Santos M, Rocha R, Florencio MH, Jennings KR. Free Radic Res 2002; 36(11): 1199-1208.
- [14] Sengupta B, Sengupta PK. Biochem Biophys Res Comm 2002; 299: 400-403.
- [15] Dufour C, Dangles O. Biochim Biophys Acta 2005; 1721: 164-173.
- [16] Sengupta B, Sengupta PK. Biopolymers 2003; 72(6): 427-434.
- [17] Falkovskaia E, Sengupta PK, Kasha M. Chem Phys Lett 1998; 297: 109-114.
- [18] Mishra B, Barik A, Priyadarsini KI, Mohan H. J Chem Sci 2005; 117(6): 641-647.